Atmospheric Environment 195 (2018) 229–242

Contents lists available at ScienceDirect

Atmospheric Environment

journal homepage: www.elsevier.com/locate/atmosenv

# Biomass and fossil fuel combustion contributions to elemental carbon across the San Francisco Bay Area

Subin Yoon[a], David Fairley[b], Tate E. Barrett[c], Rebecca J. Sheesley[a,d,*]

[a] Department of Environmental Science, Baylor University, Waco, TX, United States
[b] Research and Modeling Division, Bay Area Air Quality Management District, San Francisco, CA, United States
[c] Department of Geography and the Environment, University of North Texas, Denton, TX, United States
[d] The Institute of Ecological, Earth, and Environmental Sciences, Baylor University, Waco, TX, United States

ARTICLE INFO

*Keywords:*
Black carbon
Radiocarbon
Chemical mass balance
Emissions inventory
Source apportionment
Urban air quality

ABSTRACT

Ambient black carbon (BC) has detrimental effects on both human health and near-term global warming. To mitigate these negative effects, there have been significant efforts to reduce emissions of BC from anthropogenic and biomass burning sources in California's Bay Area since the 1960s. Recent reductions in BC have mainly been from fossil fuel combustion sources such as diesel but additional reductions may be needed for contemporary carbon sources like biomass burning and meat cooking. In this study, $PM_{10}$ (particulate matter with aerodynamic diameter of less than or equal to 10 μm) samples were collected at seven sites across the San Francisco Bay Area from November 2011 to October 2012 to create winter and non-winter composites for each site. Radiocarbon ($^{14}C$) abundance and chemical mass balance (CMB) modeling were used for source apportionment of ambient elemental carbon (EC, a proxy for BC). The $^{14}C$ abundance in the EC fraction was used to quantify the relative contributions of fossil carbon and contemporary carbon sources. The average biomass burning contributions are 48 ± 8% and 41 ± 5% for winter and non-winter seasons, respectively, across the Bay Area. Ambient concentrations of EC are approximately two to three times higher during the winter compared to the non-winter season, except for Cupertino. A CMB model, using bulk aerosol composition and select inorganic compounds, was used to understand the contributions of natural gas combustion, gasoline exhaust, and diesel exhaust to fossil carbon as well as the contribution of biomass burning and meat cooking to contemporary carbon. The different apportionment methods for EC ($^{14}C$ and CMB analysis) agree within 16 ± 12% for fraction fossil and biomass burning for both winter and non-winter seasons. The contemporary contribution to EC is much higher than estimated by current emission inventories, suggesting that the inventories may overestimate the contribution from fossil fuels, particularly diesel exhaust. The results from this study are compared to literature values from other $^{14}C$-EC or BC studies from across the world.

## 1. Introduction

Since the 1960s, significant progress has been made in the Bay Area in reducing particulate matter (PM) concentrations. Due to progressive regulations, including exhaust filters on diesel vehicles at the Port of Oakland and "no burn" days for residential fires, fine PM (aerodynamic diameter less than 2.5 μm; $PM_{2.5}$), in particular black carbon (BC) has been reduced from an annual average concentration of 4 μg $m^{-3}$ to less than 1 μg $m^{-3}$ since the late 60s (Fairley, 2012; Kirchstetter et al., 2008b, 2017). Studies have found that the reduction in BC has contributed to negative radiative forcing (i.e. cooling effect) with an overall of −1.4 $Wm^{-2}$ radiative forcing over California (Bahadur et al., 2011; Chow et al., 2010).

However, even with a threefold reduction in BC concentrations, there is still a need to understand high wintertime PM and BC concentrations and to determine which regulations would be most effective at further reducing emissions across the region. To that end, a recent year-long study was undertaken to determine source contributions to BC at seven sites across the Bay Area. Previous efforts to understand BC in the Bay Area have focused on characterization of composition and quantification of potential impacts of diesel vehicle emissions (Dallmann et al., 2011, 2013; Kirchstetter et al., 1999, 2008a). BC concentrations have been declining in the Bay Area despite an increase in diesel vehicles and fuel consumption, likely due to implementation of cleaner diesel technology (i.e. diesel particulate filters at the Port of Oakland and reductions in fuel sulfur content) and regulations

* Corresponding author. Baylor University, OBP 97266, Waco, TX, 76798, United States. Tel.: +1 254 710 3158; fax: 254 710 3409.
*E-mail address:* rebecca_sheesley@baylor.edu (R.J. Sheesley).

https://doi.org/10.1016/j.atmosenv.2018.09.050
Received 19 June 2018; Received in revised form 19 September 2018; Accepted 23 September 2018
Available online 25 September 2018

prohibiting prolonged idling of commercial diesel vehicles (~5 min) (Dallmann et al., 2011; Kirchstetter et al., 2017). With the improvement in diesel technology, it becomes more important to understand the contributions of contemporary carbon sources to BC (residential wood burning, meat cooking, agricultural burning, and wildfires) as these are also subject to increasing governmental regulations including the Bay Area Air Quality Management District's Wood-Burning Device Rule (http://www.baaqmd.gov/rules-and-compliance/wood-smoke). Approximately 38 ± 2% of households in the area contain at least one fireplace, pellet stove or wood stove (Fairley, 2014). Households also reported that burning was most likely during the winter months between November and February (McLarney and Sarles, 2005). In addition to understanding seasonal trends of emission sources, it is also of great interest to determine the spatial trends across this region, especially for regulation purposes. The sampling sites are part of the Bay Area Air Quality Management District's (BAAQMD) air pollution monitoring network and the chosen sites encompass locations (e.g. urban, residential, rural sites) that are varying distances from the coast. This study will provide better understanding in how effective regulations have been/could be across the diverse Bay Area.

Radiocarbon ($^{14}C$) analysis is used as a means of source apportionment to distinguish contribution of fossil-fuel sources, which are depleted in $^{14}C$ (half-life of $^{14}C$ is 5730 years), from biogenic sources which have a $^{14}C$ signature similar to atmospheric $^{14}C$. Source apportionment studies have used $^{14}C$ measurements to apportion total organic carbon (TOC) aerosols to distinguish between contemporary (i.e. biomass burning, meat cooking, grass pruning, detritus matter, pollen, etc.) and fossil fuel sources (i.e. diesel and gasoline exhaust, natural gas, etc.) (Barrett et al., 2015; Sheesley et al., 2012; Zotter et al., 2014b). In recent years, $^{14}C$ analysis of elemental carbon (EC) and TOC samples have been demonstrated to be a highly accurate method for quantifying contributions of fossil fuel versus biomass burning-derived EC in various locations (Barrett et al., 2015; Mouteva et al., 2017; Slater et al., 2002; Szidat et al., 2006; Zhang et al., 2014). However, very few $^{14}C$ studies of BC and EC have been reported for urban areas in the United States (U.S.) (Briggs and Long, 2016; Mouteva et al., 2017). A BC and EC source apportionment review from 2016 concluded that more studies which include inter-comparison of multiple source apportionment techniques, including $^{14}C$, chemical mass balance (CMB) and emission inventories are needed (Briggs and Long, 2016). This need for validation of apportionment methods and results is addressed in the current study by comparing results from $^{14}C$, CMB and two emissions inventories in the Bay Area following the methods listed below. This study uses EC as a proxy for BC: BC refers to measurement of light-absorbing carbon quantified by optical methods, whereas, EC refers to refractory carbon determined by physical and chemical analyses (Chow et al., 2010). $^{14}C$ measurements of EC and TOC were made to enable source apportionment of fossil vs contemporary carbon sources at seven sites across the Bay Area. CMB analysis of EC was used to increase specificity of aerosol source apportionment from fossil (diesel and gasoline vehicle emissions) and contemporary (residential biomass burning, cooking and wildfires) sources for EC. Emission inventories for California and the Bay Area were also compared to the receptor-based apportionment of EC.

## 2. Experimental methods

### 2.1. Sample collection

In accordance with BAAQMD's routine sampling, 24-h $PM_{10}$ samples were collected on a 1-in-6-day schedule at the seven sampling sites: Bethel Island, San Pablo, Concord, San Rafael, Napa, San Francisco and Cupertino (Fig. 1). All samples were collected on 8 × 10″ pre-combusted Whatman QM-A (Ann Arbor, MI, USA) quartz fiber filters (QFFs) using Anderson and TISCH high volume air samplers (Table S1 in Supplementary Material). For this study, filter samples collected during November 2011 to October 2012 were selected for analysis. Additionally, trace-gas measurements including CO and $NO_2$ were monitored using a Model 48*i* gas filter correction CO analyzer and a Model 42*i* NO-$NO_2$-$NO_x$ analyzer (Thermo Fisher Scientific, Waltham, MA, USA), respectively. These trace gas data are included in the CMB model.

### 2.2. Site description

Core Based Statistical Areas (CBSA) are geographic areas comprised of a county or counties which are socioeconomically tied to at least one urban center-based commute pattern (U.S. Census Bureau, 2012a,b). These seven sites are located in northern California and within three of the CBSAs: San Francisco-Oakland-Fremont, Santa Rosa-Petaluma, and Napa (Fig. 1). The three CBSA regions total approximately 5 million residents (U.S. Census Bureau, 2012a,b; Malone et al., 2013). The sampling sites include urban, residential, rural, and highly industrialized areas. Location of the sites vary in proximity to the coast.

- Bethel Island is a rural site with a population of 2,137 (U.S. Census Bureau, 2012a,b), producing low levels of local emissions (Malone et al., 2013). The site is ideal to measure pollutant transport between the California Central Valley and the San Francisco Bay Area. Easterly winds transport particles from the Central Valley which is one of the most productive agricultural regions in California (Malone et al., 2013; Rinehart et al., 2006).
- Concord is the largest city in Contra Costa County with a population of 122,067 (U.S. Census Bureau, 2012a,b). The city is located in the Diablo Valley. Local emission sources include major highways and two oil refineries at the north end of the valley (Claire et al., 2015). The sampling site is in a residential neighborhood (Malone et al., 2013).
- San Pablo has a population of 29,139 (U.S. Census Bureau, 2012a,b) and is heavily influenced by industry and high traffic volume including two major freeways. The sampling site is 1.2 miles downwind of the Chevron Refinery (Malone et al., 2013).
- San Rafael is the largest city in Marin County with a population of 57,713 (U.S. Census Bureau, 2012a,b). There is no industrial activity in the immediate area. However, the sampling site is close to a major transportation corridor (Malone et al., 2013).
- San Francisco is the second largest city in the Bay Area and largest among these sampling sites with a population of 805,235 (U.S. Census Bureau, 2012a,b). The densely populated city includes residents, year-round visitors and daytime commuters. The city also has some industry and has high traffic volume.
- Napa has historically had high levels of PM due to agricultural burning and fireplace use (Malone et al., 2013). It is also the largest city in Napa County with a population of 76,915 (U.S. Census Bureau, 2012a,b). The sampler at this site is situated a mile north of downtown Napa in a mixed residential and commercial neighborhood.
- Cupertino has two major highways passing through the city. This site was selected to determine the pollution impacts to residents from vehicle traffic and the Lehigh Cement Plant located one mile west of the site (Malone et al., 2013). The city has a population of 58,302 (U.S. Census Bureau, 2012a,b). The sampler was situated in Monta Vista Park (Malone et al., 2013).

### 2.3. Chemical analysis of tracers

Each $PM_{10}$ filter was analyzed for OC, EC, potassium ion ($K^+$) and chloride ion ($Cl^-$). For EC and OC analysis, filters were punched and analyzed by a thermal optical reflectance (TOR) instrument using the IMPROVE protocol (Chow et al., 1993). For $K^+$ and $Cl^-$ analysis, the ions were extracted from QFFs using deionized water and analyzed using a Dionex Ion Chromatograph (IC) System 5000 (Thermo Fisher Scientific, Waltham, MA, USA). A substantial portion of the soluble $K^+$

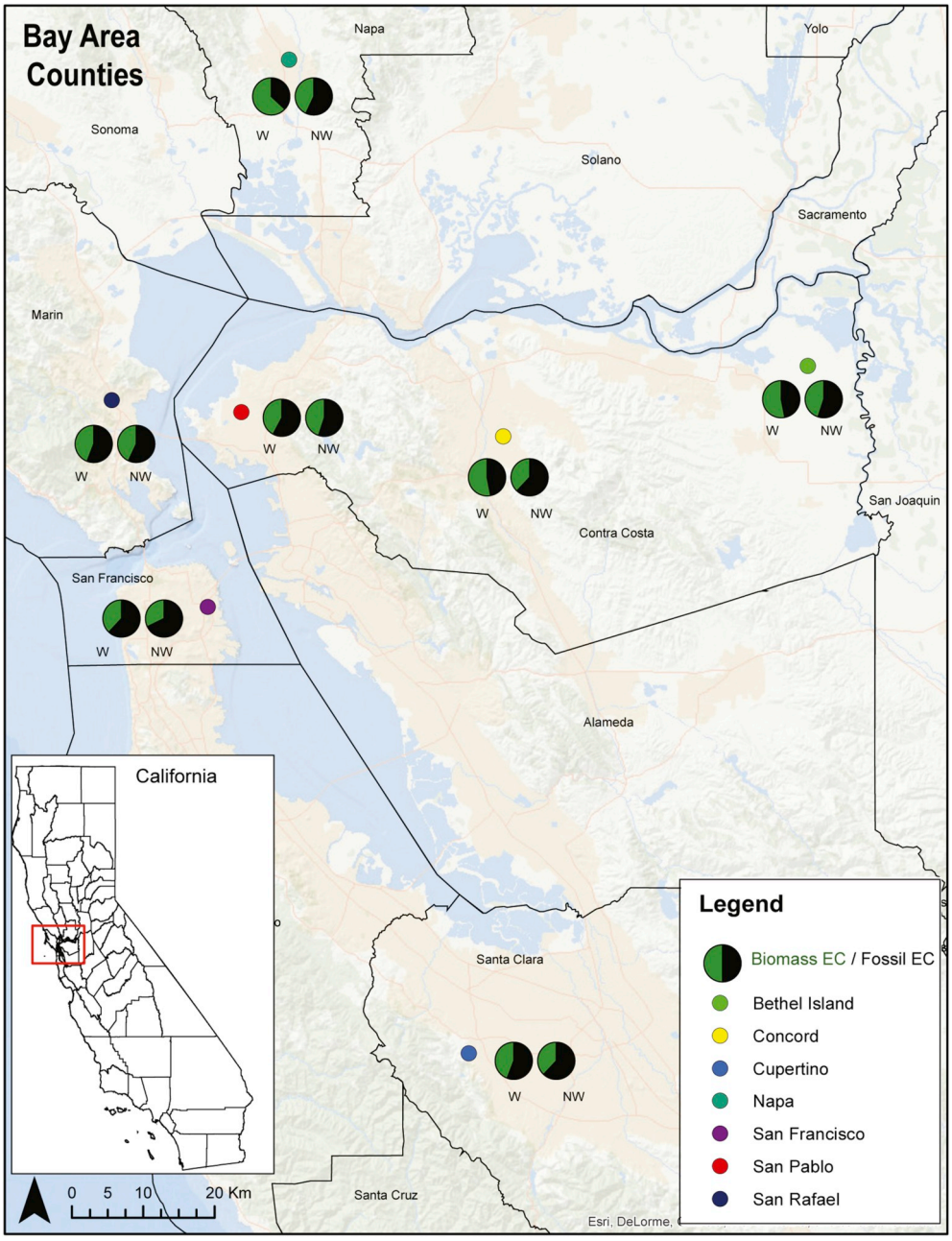


**Fig. 1.** Map of the sampling sites in the San Francisco Bay Area. Map includes sampling sites, labels and counties, county lines, and contribution of fossil fuel and biomass burning of the EC fraction for winter and non-winter season.

is from sea salt. In order to quantify the biomass burning portion, which is needed for the CMB analysis, the following equation is used to calculate non-sea salt K (nss K) (Fairley, 2012).

$$\text{nss K} = \text{K} - (0.011/0.55 * Cl) \quad (1)$$

Bulk carbon concentrations and inorganic ions were measured by the BAAQMD. All statistical analyses in this study use the Student t-test or the Mann Whitney, depending on whether the data set is symmetric or non-symmetric, respectively.

### 2.4. Description of EC composites

Two seasonal composites were established based on the need to distinguish periods of heavy firewood and biomass burning practices which are generally highest from November to February (McLarney and Sarles, 2005). Samples were separated into two periods: "winter" (November–February) and "non-winter" (March–October) composites. To obtain an equal representation of samples collected during these two seasonally different composites, a protocol was used to select seven sampling dates for each site and composite in such a way that each day of the week and month were represented as evenly as possible. Portions of each of the filters from the selected days were combined into a winter and non-winter composite for the seven sites, creating 14 composites in total. Detailed sample contributions for the composites are included in the Supplementary Material (Table S2). These samples were composited for $^{14}C$ analysis of both EC and TOC. A description of TOC sample preparation is included in the next section.

The seasonal average ambient EC concentration calculation for EC-based $^{14}C$ composites ($^{14}C$-EC) which used a mass-normalized contribution approach included equal EC mass representation from each filter sample. Each of the seven filter samples contributed approximately 15 μg of EC for a total of at least 100 μg of carbon mass – the

mass needed for $^{14}C$ analysis. The protocol ensures that the composite equally represents the source contribution from each sample, which allows understanding the average contribution of sources regardless of daily concentration. However, in order to calculate the ambient concentration of contemporary and fossil EC, a different seasonal average ambient EC concentration needs to be calculated. The average seasonal EC concentration ($Avg\ EC_{ms}$) was calculated using the following equation:

$$Avg\ EC_{ms} = \sum_{f=1}^{g} a_{fs} b_f \quad (2)$$

where $m$ is mass-based EC concentration, $s$ is the seasonal composite, $f$ is the filter sample, $a$ is the relative contribution of EC mass, and $b$ is the ambient EC concentration. The sum of the relative contribution of ambient EC concentrations from all filter samples, $g$, in $s$ represents the average seasonal EC concentration. This representation of seasonal average ambient EC concentrations is slightly different (average difference of 14 ± 5%) from a true seasonal average ambient concentration which is used for the CMB-EC and $^{14}C$-TOC measurements. The slight difference in the EC seasonal average ambient EC concentrations can be seen in Fig. 6 (B,C,E, and F) when comparing apportionment of EC using $^{14}C$ to CMB analysis.

Preliminary OC-EC runs on all samples were completed to establish the split-time for the EC harvest by the IMPROVE method. The split-time is the time when the laser reflectance of the filter is equal to the original reflectance of the filter while the instrument is operating under a He and $O_2$ atmosphere. This split-time marks the transition from combustion of OC, including pyrolyzed OC, from the filter to EC. This method operates under the assumption that pyrolyzed OC (PyrC) volatilizes prior to native EC. Once the split-time was established, the run protocol was adjusted to stop at or near the split-time, which would allow removal of the filter with isolated EC. The protocols were adjusted to harvest 82%–97% of the EC from each filter sample. Thus, the protocol is biased towards a more recalcitrant EC. There are uncertainties in this collection protocol related to PyrC, which are addressed below. Select samples were also tested for potential contribution of carbonate carbon (CC) to ambient concentration of EC. In the IMPROVE method, CC would be present in the EC4 fraction (Chow et al., 2001), so EC4 peaks in each thermogram were visually inspected and samples with the highest EC4 peaks were chosen for acid-fumigation and carbon analysis. Of these select filters, average contribution of CC to TC is at most 5 ± 5% based on seven filters across sites and seasons. The average difference in split-time is 7 ± 3 s earlier for the acid-fumigated filter, meaning that the EC isolation based on untreated split-times would be biased towards low EC recovery not towards inclusion of PryC. Because of the low contribution, and the bias towards low EC recovery in the $^{14}C$-EC samples, there is likely minimal impact of CC on the results of this study.

For the EC harvest, up to three punches of a filter sample were loaded in the analyzer at one time until a target of 100 µg of EC per composite is collected in a baked glass petri dish. Recovery of EC was tested using the number of punches from the final harvest to guarantee efficient recovery. EC recovery of each of the triple punches were from 73 to 99% while the double punches were from 84% to 98%, with no multiple punch collection resulting in the inclusion of PryC or OC. Once the EC was harvested, the filters were acid-fumigated in a desiccator over 1N hydrochloric acid (HCl) for 12 h and then dried at 60 °C for 1 h. The glass petri dishes containing each EC composite were sealed using Teflon tape, labeled, wrapped in baked aluminum foil, bagged in individual Ziploc bags and shipped on ice to National Ocean Sciences Accelerator Mass Spectrometry (NOSAMS) facility in Woods Hole Oceanographic Institution (Woods Hole, MA, USA) for $^{14}C$ analysis.

There are multiple potential sources of uncertainty in the EC $^{14}C$ method which have been discussed previously (Liu et al., 2017; Zenker et al., 2017). To understand the potential contribution of PyrC, which can be inadvertently included in the isolated EC, a sensitivity test was performed. There are published methods that correct for the potential bias including a water extraction pretreatment prior to EC isolation. However, this method has documented up to 20% loss of EC due to the extraction (Dusek et al., 2014). For this study we used another protocol which conducts a post-analysis sensitivity test to report bias of PyrC if included in the $^{14}C$ of isolated EC (Andersson et al., 2015; Budhavant et al., 2015; Chen et al., 2013). Results from this test calculate a maximum underestimation of fossil contribution to EC by 8.5 and 9.9% for winter and non-winter samples, respectively. To incorporate potential carbon contamination from shipping and handling of the EC harvested samples, a separate sensitivity test was conducted. Several blank filters were prepared replicating a similar EC harvest sample (e.g. volatilized off OC by heating the sample, acid fumigation, drying, etc.), and shipped and handled using the same method as the EC harvested ambient samples. These travel blanks were then analyzed for carbon contamination using the carbon analyzer. The average contribution of contaminated carbon on the travel blanks is 0.09 ± 0.08 µg cm$^{-2}$. A maximum $^{14}C$ contribution from this contaminated carbon mass is calculated assuming the carbon to be pure fossil (−1000‰) or pure biomass burning (+107.5‰). Results from this test indicate a maximum percent difference of $^{14}C$ of the EC due to blank subtraction of 2.5 and 11.3% for winter and non-winter samples, respectively. The results from both sensitivity tests, potential contribution of PryC during EC harvest, and potential contribution of contaminated carbon during shipping and handling, were combined to calculate the uncertainty of $^{14}C$ of the ambient samples.

### 2.5. Description of TOC composites

Sample preparation for $^{14}C$ analysis of the TOC composite samples was completed at the BAAQMD. As with the EC composite samples, the TOC samples were separated into two composites: “winter” (November–February) and “non-winter” (March–October). These composites were composed of the same filter samples as the EC composites, using equal area from each filter (Table S2).

The TOC composite samples and a $PM_{10}$ filter blank were sent to University of Arizona Accelerator Mass Spectrometry Laboratory (Tucson, AZ, USA) where carbon isotope analysis was performed. The $^{14}C$ results of the TOC sample composites were blank corrected, using $^{14}C$ results from the filter blank, to account for potential contamination of carbon from shipping and handling of the samples.

### 2.6. Method for radiocarbon analysis

The sample composites were first oxidized to $CO_2$, purified and quantified by manometry. Samples were then reduced to graphite and subjected to accelerator mass spectrometry (AMS) to determine the fraction of modern carbon ($F_M$) which is the $^{14}C/^{12}C$ ratio of the sample to the “Modern” or a reference material: NBS Oxalic Acid I (in AD 1950) (Stuiver and Polach, 1977).

$$F_M = \frac{(^{14}C/^{12}C)_{sample}}{(^{14}C/^{12}C)_{AD1950}} \quad (3)$$

### 2.7. Source apportionment modeling

#### 2.7.1. Radiocarbon-based apportionment

For apportionment, the $F_M$ value is used to calculate the $\Delta^{14}C_{sample}$ for the EC and TOC samples.

$$\Delta^{14}C_{sample} = 1000 * (F_M * exp((1/8267) - (1950 - 2012)) - 1) \quad (4)$$

The isotope signature can be apportioned between fossil fuel and biomass burning by using a mixing model ratio for $\Delta^{14}C_{sample}$ with end members specific to these sources:

$$\Delta^{14}C_{sample} = (\Delta^{14}C_{contemporary})(f_M) + (\Delta^{14}C_{fossil})(1 - f_M) \quad (5)$$

The $\Delta^{14}C_{fossil}$ component of $\Delta^{14}C_{sample}$ has a value of −1000‰ while $\Delta^{14}C_{biomass\ burning}$ can be between +28.1‰ (Zotter et al., 2014b) and +102.5‰. The +102.5‰ corresponds to the end member value of EC from wood smoke which was derived from averaging sections of an 80-year-old pinewood from the Bay Area. This was based on an auxiliary study in collaboration with BAAQMD. The calculated end member value from this auxiliary study (+102.5‰) is similar to a published wood smoke end member value (+107.5‰) which was derived from a tree growth model by averaging 10–85 year old wood fractions (Mohn et al., 2008). The $^{14}C$ value of +28.1‰ corresponds to biomass burning of annual sources including combustion of grass, pruning, and agricultural waste, as well as meat cooking (Zotter et al., 2014b). A bottom-up approach using the BAAQMD's 2011 Emissions Inventory (EI) for Criteria Air Pollutants was employed to calculate a $\Delta^{14}C_{biomass\ burning}$ end member value specific to its region and season (Fanai et al., 2014).

$$\Delta^{14}C_{biomass\ buring} = (f_{wood\ smoke})(+102.5\%) + (f_{annual\ biomass\ buring})(+28.\ 1\%) \quad (6)$$

The Bay Area-tailored $\Delta^{14}C_{biomass\ burning}$ end member for winter and non-winter periods were calculated to be +98.5‰ and +71.2‰, respectively. This customized end member is also applied for the $^{14}C$ analysis of the TOC samples.

#### 2.7.2. Chemical mass balance modeling

To further apportion sources of fossil fuel and biomass burning, CMB analysis using a Monte Carlo source apportionment technique was employed to determine contribution of major sources collected on sampled $PM_{10}$ filters. The CMB is a receptor-based model that uses known speciated source profiles to identify sources and source contribution to carbonaceous aerosol. The model uses the following set of linear equations to estimate the $c_{ik}$ which is the concentration of elemental carbon, $i$, at receptor site $k$:

$$c_{ik} = \sum_{j=1}^{m} f_{ij} s_{jk} \quad (7)$$

which equals the sum of $m$ source types where $s_{jk}$ is the contribution to the ambient elemental mass concentration from source $j$ at receptor site $k$, and $f_{ij}$ is the relative concentration of chemical component $i$ in the emissions from source $j$. In this analysis, the standard deviation of the measured and model estimated masses is determined by using a Monte Carlo approach. This technique repeatedly samples from the profile distribution (approximately 100,000 times).

The CMB analysis relied on measurements of OC, EC, $^{14}C$-EC, $^{14}C$-OC and nss K from the filters, and 24h average $NO_x$ and CO measurements. The $^{14}C$-OC values were determined using $^{14}C$-TOC and $^{14}C$-EC values (Supplementary Material). Profiles from five source categories were used: gasoline, diesel, natural gas, biomass burning, and cooking (Fairley, 2012; Fanai et al., 2014). These five sources account for over 90% of directly emitted carbonaceous $PM_{2.5}$ and nearly 100% of EC, based on the BAAQMD's EI. These sources are also commonly used in other urban source apportionment studies (Fraser et al., 2003; Mohr et al., 2009; Rogge et al., 1991; Schauer et al., 1996; Zheng et al., 2002). Except for wood smoke/biomass burning, the same profiles were used for the winter and non-winter composite analysis. During the winter season biomass burning is predominately from wood smoke while the non-winter season had similar contributions from wood smoke and annual biomass burning. For the winter season, a source profile of wood smoke was used while a combined wood smoke and annual biomass burning profile was used for the non-winter season. However, for the CMB analysis we will report apportioned wood smoke and/or biomass burning as "wood smoke". The term "biomass burning", when discussing the CMB analysis, will refer to combined "wood smoke" and "cooking" sources.

## 3. Results and discussion

### 3.1. Bulk carbon concentrations and OC to EC ratios

The ambient concentrations of OC and EC composites during the winter ranged from 1.29 to 8.67 μg $m^{-3}$ and 0.23 to 2.77 μg $m^{-3}$, respectively, while non-winter samples ranged from 1.21 to 3.70 μg $m^{-3}$ and 0.35 to 0.45 μg $m^{-3}$, respectively (Table 1). For both seasons, Napa consistently had the highest concentrations of OC and EC while Cupertino and San Pablo had the smallest in the winter and non-winter season, respectively. It was initially thought that Bethel Island would be a background site, but inland sources (i.e. Central Valley) kept carbonaceous aerosol concentrations relatively high. Ambient concentrations of OC and EC were significantly enhanced ($p < 0.05$) in the winter versus non-winter samples for Bethel Island, San Rafael, Napa and San Francisco. San Pablo had a significantly enhanced ambient OC concentration ($p < 0.05$) during the winter season, however there was no significant difference ($p = 0.05$) in the EC concentration during the two seasons. Concord had no significant difference ($p = 0.07$) of ambient OC concentration between the two seasons, but the EC concentration was more enhanced ($p < 0.05$) during the winter season. For Cupertino, there was no significant difference between the two seasons for

**Table 1**
Average (mean standard deviation) ambient EC and TOC concentrations for each composite sample. Isotope analysis including $\Delta^{14}C$ and $\delta^{13}C$ (‰), contribution biomass burning (%BB) or contemporary (%Cont) for EC harvest and TOC samples, respectively, are included in the table.

| Locations | Ambient Concentration | | | EC | | | TOC | | |
|---|---|---|---|---|---|---|---|---|---|
| | Composite | EC (μg $m^{-3}$)[a] | TC (μg $m^{-3}$) | $\Delta^{14}C$ (‰) | $\delta^{13}C$ (‰) | %BB | $\Delta^{14}C$ (‰) | $\delta^{13}C$ (‰) | %Cont |
| Bethel Island | Winter | 0.79 ± 0.09 | 6.10 ± 3.00 | −415.7 | −25.74 ± 0.22 | 53 ± 6 | −257.4 | −26.01 ± 0.02 | 68 ± 6 |
| | Non-Winter | 0.32 ± 0.06 | 2.99 ± 1.05 | −516.6 | −27.14 ± 0.13 | 45 ± 10 | −333.8 | −26.89 ± 0.02 | 62 ± 7 |
| Concord | Winter | 0.73 ± 0.08 | 4.93 ± 5.05 | −414.4 | −26.12 ± 0.25 | 53 ± 7 | −264.4 | −26.08 ± 0.01 | 67 ± 6 |
| | Non-Winter | 0.36 ± 0.07 | 3.06 ± 1.11 | −591.1 | −26.91 ± 0.15 | 38 ± 11 | −378.7 | −26.99 ± 0.03 | 58 ± 6 |
| San Pablo | Winter | 0.72 ± 0.08 | 4.97 ± 1.90 | −537.3 | −26.00 ± 0.20 | 42 ± 7 | −381.8 | −26.13 ± 0.01 | 56 ± 4 |
| | Non-Winter | 0.37 ± 0.07 | 2.52 ± 0.92 | −522.2 | −24.96 ± 0.13 | 45 ± 14 | −496.5 | −26.73 ± 0.05 | 47 ± 3 |
| San Rafael | Winter | 0.79 ± 0.09 | 5.36 ± 2.69 | −518.5 | −25.61 ± 0.25 | 44 ± 8 | −339.3 | −26.33 ± 0.01 | 60 ± 5 |
| | Non-Winter | 0.36 ± 0.07 | 3.04 ± 0.62 | −534.1 | −25.65 ± 0.12 | 44 ± 8 | −317.6 | −26.91 ± 0.06 | 64 ± 8 |
| San Francisco | Winter | 0.94 ± 0.09 | 5.75 ± 2.63 | −577.1 | −24.47 ± 0.21 | 39 ± 7 | −426.6 | −26.32 ± 0.01 | 52 ± 3 |
| | Non-Winter | 0.37 ± 0.07 | 2.82 ± 1.13 | −661.5 | −25.74 ± 0.13 | 32 ± 13 | −445.3 | −26.70 ± 0.01 | 52 ± 4 |
| Napa | Winter | 1.34 ± 0.11 | 8.95 ± 2.91 | −308.0 | −25.13 ± 0.15 | 63 ± 9 | −137.3 | −25.98 ± 0.01 | 79 ± 7 |
| | Non-Winter | 0.40 ± 0.07 | 3.59 ± 1.28 | −544.5 | −25.90 ± 0.14 | 43 ± 8 | −364.9 | −26.49 ± 0.02 | 59 ± 5 |
| Cupertino | Winter | 0.50 ± 0.07 | 4.08 ± 1.79 | −515.0 | −25.21 ± 0.21 | 44 ± 5 | −405.2 | −26.38 ± 0.01 | 54 ± 4 |
| | Non-Winter | 0.38 ± 0.07 | 3.06 ± 1.01 | −597.2 | −26.20 ± 0.14 | 38 ± 10 | −413.4 | −26.60 ± 0.01 | 55 ± 4 |

[a] Mass-normalized composite.

either OC ($p = 0.29$) or EC ($p = 0.19$). The seasonal trend observed from some of the sampling sites (i.e. higher carbonaceous aerosol concentration during the winter versus non-winter season) has historically been observed in the Bay Area (Kirchstetter et al., 2017) and can be partially explained by meteorological factors (i.e. wind speed, mixing heights, etc.). Glen et al. observed dispersion of pollutants to be 2 to 3 times stronger in the summer (May–August) than the winter in the Bay Area (Glen et al., 1996). In addition to meteorological influences, residential wood burning significantly impacts wintertime air quality in this region (McLarney and Sarles, 2005).

EC (or BC) is a highly stable, combustion byproduct that is directly emitted into the atmosphere from combustion sources (Strader et al., 1999; Turpin and Huntzicker, 1995). Particulate OC can be directly emitted (primary OC), but can also be produced in the atmosphere via chemical reactions of precursor volatile organic compounds (secondary OC). Primary OC is also less stable in the atmosphere with respect to chemical reactions, compared to EC. Using the ratio of OC to EC provides a qualitative measure of the impact of these secondary compounds, which are referred to as secondary organic aerosols (SOA) (Turpin and Huntzicker, 1995). An increase in the OC to EC ratio may indicate an increase in SOA contribution, while a high correlation between OC and EC may indicate that primary combustion emissions dominate the aerosol.

During the winter, OC more strongly correlates to EC ($r^2 = 0.85$) (Fig. 2A) compared to the non-winter season ($r^2 = 0.56$) (Fig. 2B), however, this may be due to greater range of concentrations in the winter season producing higher correlation. The average OC to EC ratios are 4.5 and 6.2 during the winter and non-winter season, respectively. All sampling sites, except San Pablo ($p = 0.59$) and Cupertino ($p = 0.25$), registered significantly higher OC to EC ratios during the non-winter versus winter season ($p < 0.05$) (Fig. 3). The largest average OC to EC ratio was at Bethel Island ($7.33 \pm 1.12$) during the non-winter period. The smallest average OC to EC was at San Francisco ($3.83 \pm 0.96$) in the winter. For the Bay Area samples, the higher OC to EC ratio during the non-winter season is supporting evidence that the winter OC and EC are likely from combustion sources, while non-winter OC is mostly more influenced by SOA production (Turpin et al., 1991).

Since SOA is a subset of carbonaceous aerosols formed via reactions of volatile and intermediate volatility precursors with atmospheric oxidants like ozone, hydroxyl radical, or nitrate radicals (Kleindienst et al., 2007), correlations of OC to ozone were used to further investigate whether increased OC to EC ratio is due to SOA. Production of ozone is largely dependent on meteorology (i.e. warmer temperature, stagnant air masses and clear skies), with mixing ratios higher during summer months. A stronger correlation is observed between OC and 8-hr max ozone concentration during the summer season ($r^2 = 0.46$: slope = 12.9) (Fig. 4) compared to the winter season ($r^2 = 0.17$). The higher OC to EC ratios collected during the non-winter season (March to October) and correlation between ozone and OC during the summer (subset of non-winter samples) season (May to August) point to higher impacts of SOA in the non-winter season. However, average OC to EC ratios in the Bay Area during the non-winter season were less than half the average ratio observed during summer months in Nashville, TN ($12.11 \pm 5.50$), an area with high biogenic SOA impacts (Lewis et al., 2004).

### 3.2. Source apportionment studies

#### 3.2.1. Radiocarbon analysis of TOC

Contemporary contributions to TOC include combustion (e.g. biomass burning and cooking), biogenic (e.g. vegetative detritus), and secondary sources. During the winter season, TOC composites had significantly larger ($p < 0.05$) contribution of contemporary ($62 \pm 9\%$) compared to fossil fuel sources ($38 \pm 9\%$) (Fig. 5A and D). Average ambient concentrations from contemporary and fossil fuel sources during the winter season were $3.67 \pm 1.59\,\mu g\,m^{-3}$ and $2.06 \pm 0.35\,\mu g\,m^{-3}$ of TOC, respectively. Napa had both the largest contribution ($79 \pm 7\%$) and ambient concentration ($7.03 \pm 0.65\,\mu g\,m^{-3}$) from contemporary sources. San Francisco had the largest contribution ($48 \pm 3\%$) and ambient concentration ($2.75 \pm 0.20\,\mu g\,m^{-3}$) from fossil fuel sources during the winter season.

The non-winter TOC samples also had a statistically larger ($p < 0.05$) contribution of contemporary ($57 \pm 6\%$) compared to fossil fuel ($43 \pm 6\%$) sources. Fossil fuel and contemporary contribution sources are closer to equal parts during the non-winter season, although the two seasons are not significantly different ($p = 0.12$). Average ambient TOC concentrations for contemporary and fossil fuel sources were $1.72 \pm 0.32$ and $1.29 \pm 0.13\,\mu g\,m^{-3}$, respectively. Though Bethel Island had the largest contribution from contemporary sources ($62 \pm 7\%$), ambient concentrations from contemporary sources were largest in Napa ($2.14 \pm 0.19\,\mu g\,m^{-3}$). San Pablo had largest contribution from fossil fuel sources ($53 \pm 3\%$), however Napa had the largest ambient concentration ($1.46 \pm 0.20\,\mu g\,m^{-3}$) of TOC from fossil fuel sources.

For both winter and non-winter TOC composites, contemporary sources are the dominant contributor of carbonaceous aerosols. Napa has significantly more contemporary carbon compared to other sampling sites, especially during the winter season. The Napa sampling site is in the center of Napa Valley where agricultural burning and fireplace usage during fall and winter are more frequent. During the winter season, as expected, the urban San Francisco site was the most impacted by fossil fuel sources (Fig. 5A). San Francisco also had the same fossil fuel contribution (48%) in both season composites. The San Francisco winter composite had the largest fossil fuel contribution while the non-

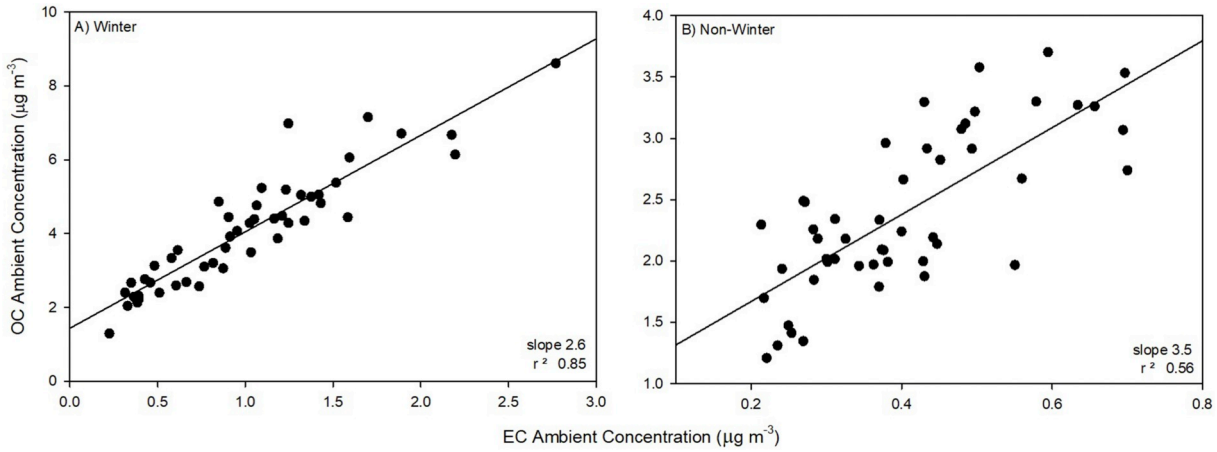


**Fig. 2.** Correlation of ambient OC and EC concentrations for (A) winter and (B) non-winter samples.

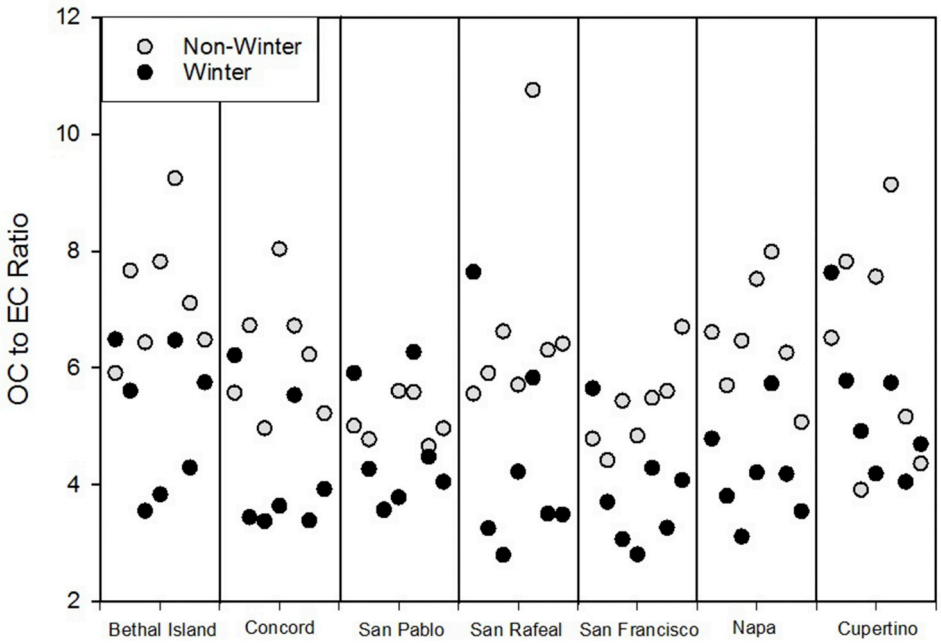


**Fig. 3.** Comparison of OC to EC ratio for winter and non-winter samples specific to each sampling site.

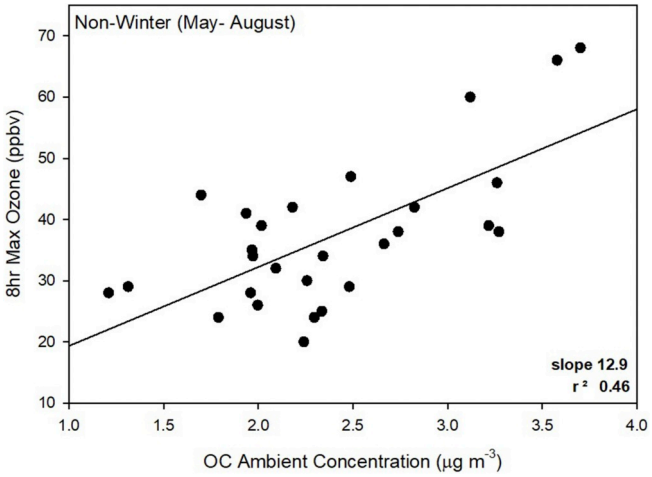


**Fig. 4.** Correlation of 8hr ozone max to ambient OC concentrations on days sampled during months May through August.

winter composite has second largest fossil fuel contribution after San Pablo (53 ± 3%) which is considered an outlier. The average contribution from contemporary sources of TOC aerosols in the Bay Area (59 ± 8%) was comparable to other major Californian cities including Pasadena, where average summer contribution of contemporary sources is 51 ± 15% (Zotter et al., 2014b). However, ambient concentrations from contemporary sources were generally greater in Pasadena (2–4 $\mu g\,m^{-3}$) (Zotter et al., 2014b) compared to the Bay Area (~2 $\mu g\,m^{-3}$).

### 3.2.2. Radiocarbon analysis of EC

As EC is from combustion processes, the contemporary contribution of EC includes sources from biomass burning and cooking. These sources will be referred to as "biomass burning" for the $^{14}$C-EC analysis. During the winter season, average contributions from biomass burning and fossil fuel sources were 48 ± 9% and 52 ± 9%, respectively. Unlike the TOC composite samples, there was no statistically significant difference ($p = 0.42$) between fraction of biomass burning and fossil fuel sources in the EC samples during the winter season across the sites. However, there was a significant difference ($p < 0.05$) between EC apportioned to biomass burning and fossil fuel sources during the non-winter season, where average biomass burning contributions (41 ± 5%) were significantly smaller compared to fossil fuel contributions (59 ± 6%). During the winter, average ambient EC concentrations from biomass burning and fossil fuel sources were 0.41 ± 0.20 and 0.42 ± 0.10 $\mu g\,m^{-3}$, respectively. Average ambient concentrations during the non-winter season for biomass burning and fossil fuel sources were 0.15 ± 0.02 and 0.22 ± 0.03 $\mu g\,m^{-3}$, respectively. For the winter season, Napa had the largest contribution and ambient concentration of EC from biomass burning during the winter: 63 ± 9% and 0.84 ± 0.12 $\mu g\,m^{-3}$, respectively. San Francisco had the largest contribution and ambient concentration of EC from fossil fuel: 61 ± 7% and 0.58 ± 0.07 $\mu g\,m^{-3}$, respectively. For the non-winter season, Bethel Island had the largest contribution of EC from biomass burning: 45 ± 10%, while the largest ambient EC concentration from biomass burning was from Napa: 0.17 ± 0.03 $\mu g\,m^{-3}$. Bethel Island likely received transport of biomass burning pollutants from Central Valley where there is heavy agricultural activity. Consistent with the winter, San Francisco had the largest contribution and ambient concentration of EC from fossil fuel during non-winter season: 68 ± 13% and 0.25 ± 0.05 $\mu g\,m^{-3}$, respectively.

Major sources of EC in this region have historically been from on- and off-road diesel exhaust (Bond et al., 2004; Kirchstetter et al., 2017). A major source of future EC may be from wildfires, as studies have found increasing trends and projections of large-scale fires in California (Barbero et al., 2015; Riley et al., 2013; Westerling et al., 2006). However, a study by Schauer and Cass (2000) of California carbonaceous aerosol samples collected over 15 years prior to this study, found that even with the inclusion of a major wildfire events, biomass burning contributed only 20% of EC (Schauer and Cass, 2000). From our results, with the large decrease in emissions of EC from diesel, there is evidence that biomass burning, and potentially meat cooking, are becoming more prominent contributors to EC or BC concentrations. These trends are also observed in the TOC samples, aside from the outlier (i.e. non-winter San Pablo composite). Contributions from the winter season show an overall equal contribution of biomass burning and fossil fuel combustion sources for EC amongst the seven sampling sites (Fig. 5B and E). Although non-winter samples have statistically higher contributions from fossil fuel sources, average biomass burning (40 ± 5%)

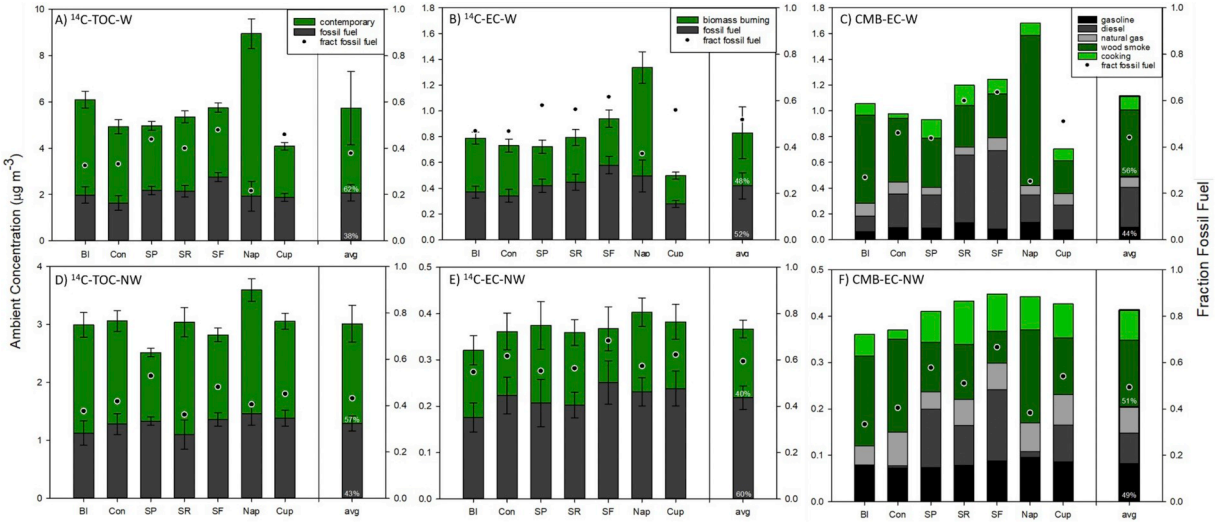


**Fig. 5.** Ambient concentration of fossil fuel and contemporary sources using radiocarbon-based source apportionment of (A) winter TOC samples, (D) non-winter TOC samples, (B) winter EC samples, and (C) non-winter EC samples. Ambient concentration of fossil fuel (e.g. gasoline, diesel, and natural gas), wood smoke, and cooking sources for (C) winter and (F) non-winter EC samples using chemical mass balance-based apportionment. Fraction (fract) fossil fuel is included in each graph.

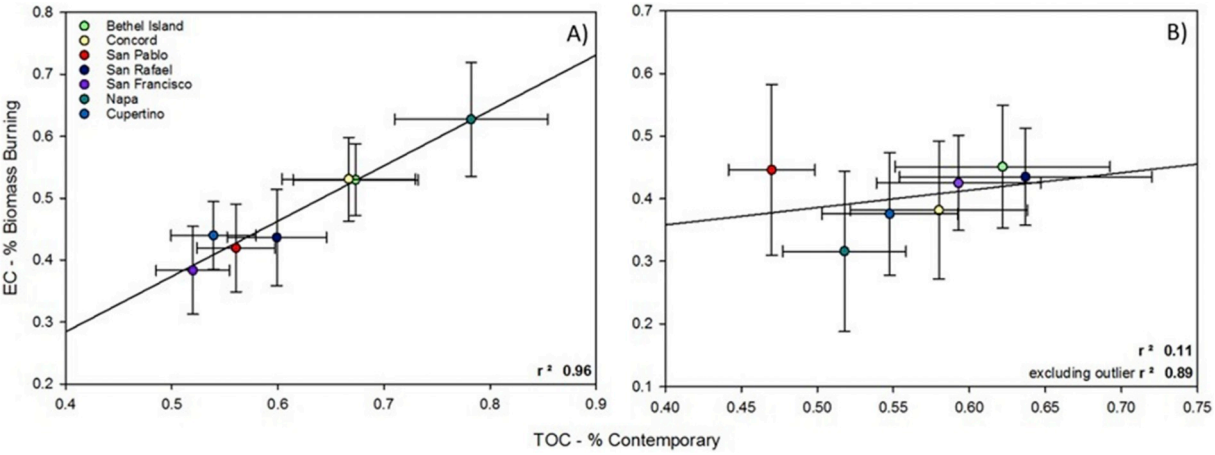


**Fig. 6.** Comparison of contribution of biomass burning from EC harvested composite samples to contribution of contemporary sources from TOC composite samples for (A) winter and (B) non-winter seasons.

contributions from all sites were still much larger than the estimated 20% from the Schauer and Cass (2000) study.

Based on the State of California's Cal Fire website (http://cdfdata.fire.ca.gov/incidents/incidents_seasondeclarations?year=2012), summer and winter wildfire seasons in northern California begin approximately in May and November, respectively. During the period of this study, however, there were few recorded large fires in the region (CAL FIRE, 2012). Thus, the enhanced concentrations from biomass burning in this study derive from residential wood burning and possibly some agricultural burning. The EC contribution from biomass burning during the winter season is significantly ($p = 0.03$) greater compared to the non-winter season. There is also a strong correlation between the biomass burning (EC composite) and contemporary (TOC composite) sources during the winter ($r^2 = 0.96$) and non-winter ($r^2 = 0.89$, excluding the San Pablo outlier) season (Fig. 6). The strong correlations during the two seasons are an indication that the biomass burning contribution from the EC fraction and the contemporary OC are from the same source or combination of common sources. However, as the non-winter OC to EC ratios are greater, these aerosols are likely more impacted by secondary OC sources.

### 3.2.3. Chemical mass balance apportionment of EC

The apportionment of EC is different between the CMB and $^{14}C$ analysis (Fig. 5B–C, 5E-F). The CMB analysis uses volume-normalized contributions (same method as the TOC $^{14}C$) to calculate average EC mass for each sample site. The $^{14}C$ analysis calculates average EC by equal mass representation. Due to the difference in average EC calculation method per site, an average of 14 ± 6% higher EC ambient concentration is present in the CMB apportionment. For the CMB analysis, EC was apportioned to three fossil fuel sources (i.e. gasoline exhaust, diesel exhaust, and natural gas) and two biomass burning sources (i.e. wood smoke and cooking) (Fig. 5C and F). The relative contributions of EC from the CMB and $^{14}C$ source apportionment analysis can be easily compared.

During the winter season, the average estimated contributions from fossil fuel and biomass burning sources were 45 ± 15% and 55 ± 15%, respectively, for CMB. Contributions of natural gas (8 ± 3%) and gasoline (9 ± 2%) were relatively consistent across the sites. The largest contribution of fossil EC is diesel exhaust with an average contribution of 28 ± 14%. San Francisco had the highest ambient concentration of diesel exhaust at 0.61 ± 0.12 µg $m^{-3}$. Wood smoke dominates the

biomass burning fraction of EC with an average of 45 ± 17% contribution to winter EC concentrations. Napa had the highest ambient concentration of biomass burning at 1.16 ± 0.23 μg $m^{-3}$ and the highest contribution 69 ± 3%.

During the non-winter season, average contributions from fossil fuel and contemporary sources are 49 ± 12% and 51 ± 12%, respectively, for CMB. The largest contribution of fossil EC in the non-winter season was from gasoline exhaust with an average of 20 ± 2% amongst the sites. Contribution of gasoline exhaust was also consistent across the sites like in the winter season. Diesel exhaust was quite variable throughout the region, with San Francisco having the largest contribution and ambient concentration with 34% and 0.15 μg $m^{-3}$, respectively, whereas for Bethel Island, the CMB analysis apportioned no contribution of carbonaceous aerosols to diesel exhaust. As with the winter season, biomass burning also dominated the contemporary combustion fraction of EC during the non-winter season. Average contribution and concentration of biomass burning was 36 ± 15% and 0.14 ± 0.05 μg $m^{-3}$. The largest contribution and ambient concentration of biomass burning was from Napa with 45% and 0.20 μg $m^{-3}$, respectively.

Ambient concentrations of all sources were significantly ($p < 0.05$) enhanced in the winter versus non-winter season, aside from the gasoline exhaust ($p = 0.26$). Ambient concentrations of gasoline exhaust remained consistent throughout the seasons proving that this is not a seasonally influenced source like residential wood smoke (i.e. biomass burning). The relative contribution of gasoline exhaust was enhanced during the non-winter season ($p < 0.05$), however, this was likely due to decrease of overall aerosol concentrations during this season.

### 3.3. Comparison of source apportionment methods

The different apportionment methods, $^{14}C$ and CMB analysis for EC, agree within 16 ± 12% for contribution of fraction fossil and biomass burning for both winter and non-winter season. Samples from Bethel Island and Napa consistently had larger differences between the two analysis methods for both seasons. Both sites had significant contributions from contemporary sources. Interestingly, CMB analysis consistently over-predicted the contemporary contribution by an average of 9 ± 9%. The CMB analysis uses nss K as the only tracer for biomass burning. Though nss K is a stable compound and resistant to chemical degradation, the ion is not a unique tracer for biomass burning and adds uncertainty in the apportionment.

### 3.4. Comparison to emissions inventory data

California Air Resources Board's Black Carbon Emission Inventory (CARB-EI) reports statewide speciation of EC from its different sources (CARB, 2016). The CARB-EI estimates that on-road motor vehicle exhaust contributes 20% of total EC emissions (18% from diesel and 2% from gasoline) while off-road mobile sources (e.g. aircraft, off-road equipment, commercial harbor craft, and trains) contribute 36% of total EC (Fig. 7). The combined total of off-road mobile and on-road gasoline and diesel sources contribute 56% of total EC emissions which closely aligns to the $^{14}C$-EC analysis: average fossil fuel contribution of EC is 56 ± 8%. However, if EC from industrial sources (i.e. petroleum production, wood and paper, mineral processes) is included as fossil fuel, then the CARB-EI estimates 70% contribution of EC from all mobile plus industrial sources, which is significantly higher than the $^{14}C$-EC average.

The CARB-EI is an average estimate of the contribution of EC from across the state of California. The BAAQMD has published the Bay Area Emissions Inventory for $PM_{2.5}$ (BAAQMD-EI) (Claire et al., 2015) providing detailed speciation for $PM_{2.5}$ specific to the sampling region. The contribution of EC by fuel type was calculated for this paper using the BAAQMD-EI and EPA's factors for estimating the fraction of $PM_{2.5}$ to BC (Fig. 7), however, this may be uncertain with regards to BC source ratios and number of source types. This calculation estimates that fossil fuel sources contribute 76% of total EC emissions: 44% from diesel, 8% from gasoline and 24% from natural gas. The CMB-EC analysis estimates lower fossil fuel contributions from diesel (22 ± 15%) and natural gas (11 ± 4%). However, the contribution of EC from gasoline exhaust is larger in the CMB analysis (14 ± 6%) compared to the BAAQMD-EI (2%). This may be due to underestimation of high emitters within the gasoline exhaust category in the emissions inventory (Lough et al., 2007).

The BAAQMD-EI estimates contemporary sources to contribute 15% of EC emissions including 14% from wood smoke and 1% from cooking. The CARB-EI estimates that contemporary sources contribute 22% of EC emissions, including 15% from residential wood smoke, 4% from cooking, and 3% from agricultural burning (Fig. 7). The $^{14}C$-EC analysis estimates a contribution from contemporary sources (44 ± 8%) larger than either EIs. The CMB-EC analysis estimates larger contributions from wood smoke (41 ± 16%) and cooking sources (13 ± 5%) compared to the EIs (Fig. 7). The CMB and $^{14}C$ apportionment analysis for EC has a considerably larger contribution of EC from contemporary, wood smoke and cooking emissions compared to the EI. In summary, the EIs consistently predict lower contributions from biomass burning as compared to receptor-based techniques ($^{14}C$ and CMB). However, differences in the EI and observation-based apportionment can be partially due to differences in methodology of bottom-up (i.e. EI models) and top-down (receptor-based) approaches.

### 3.5. Comparison of radiocarbon-based EC results to other studies

To assess how source contributions to EC in the Bay Area of California compares to other locations, a review of the current literature for global $^{14}C$ studies of BC and EC was completed. Table 2 includes $^{14}C$ apportionment of EC or BC, by method and season, from across the globe. The region with the most $^{14}C$ EC and BC studies is Asia, followed by Europe, the Artic, and finally, the contiguous U.S. (Table 2). At the time of this publication, there has been only one other study in the contiguous U.S., by Mouteva et al. in Utah, (2017). There are no reported studies in the Southern Hemisphere. Fig. 8 and Figure S1 (Supplementary Material) plot the $^{14}C$ apportioned EC or BC data on a global map for the winter and non-winter (and annual) seasons, respectively. Regional trends in the contribution of biomass burning to EC or BC can be visualized using these global maps (Fig. 8 and S1). In Asia, studies can be grouped between East (i.e. China, South Korea, and Japan) and South (i.e. India, Maldives, and Himalaya-Tibet) Asia. Generally, there is a larger contribution of fossil fuel combustion to EC and BC in East Asia, while South Asia has a larger contribution of biomass burning. There is significant variability across the many European studies and the two contiguous U.S. studies.

Looking in more detail at Table 2, the average winter season contribution of biomass burning is 48 ± 8% for the Bay Area sites, with relatively little variability amongst the study sites. The European-based EC apportionment studies report highly varying contribution (4–99%) from biomass burning sources overall for winter. However, the average winter season in the Bay Area is most comparable to winter measurements in Switzerland (%BB of 25–63%; excluding Moleno where contribution of EC was dominated by fossil fuel sources at a %BB of 4–18%). Overall winter measurements in East Asia (%BB: 12–43%) had a lower EC and BC contribution from biomass burning compared to the Bay Area and the European sites. The consistently high contribution of fossil fuel combustion derived-EC in China is likely due to prominent usage of coal combustion (Cao et al., 2011a,b; Huang et al., 2014). Relative to East Asia, South Asia had higher contribution from biomass burning (41–59%), which is more comparable to measurements in the Bay Area. Biomass burning, especially during the winter, is likely influenced by residential, biofuel and agricultural burning in South Asia (Bond et al., 2004; Stone et al., 2010). In the Bay Area, the average contribution of biomass burning is lower in the non-winter season (41 ± 5%). This pattern is also seen in the European studies (excluding

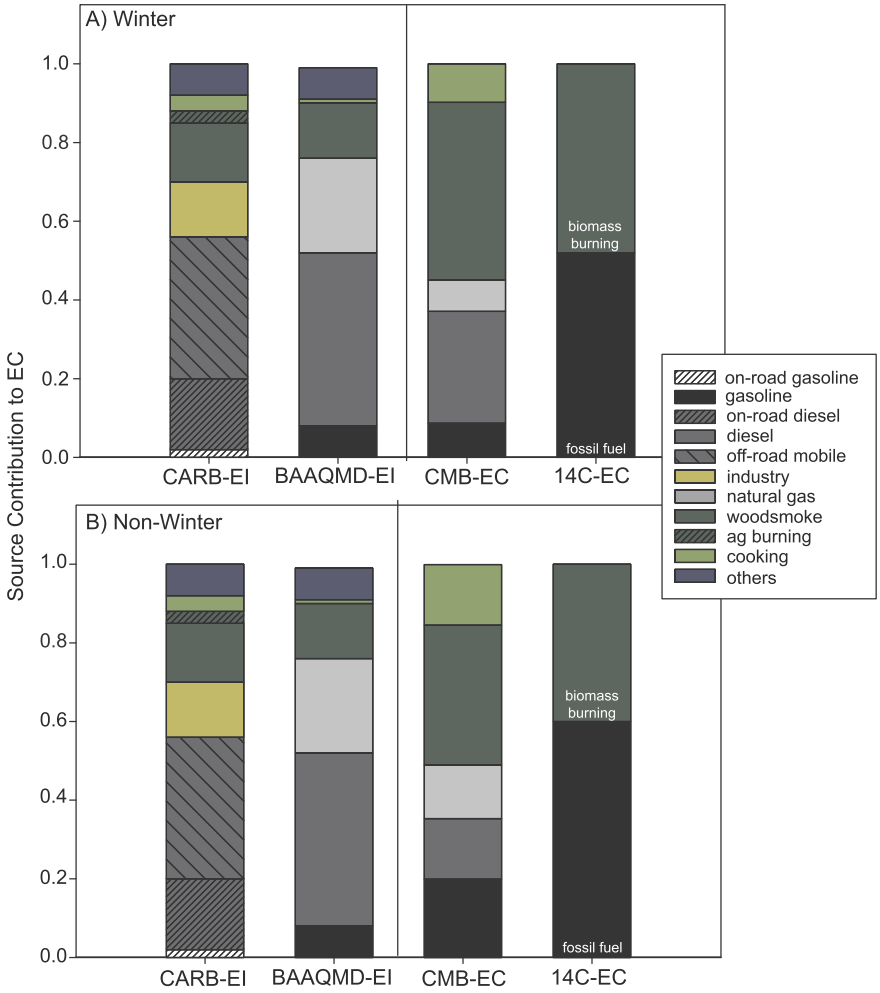


**Fig. 7.** Comparison of estimated source contribution of EC based on CARB's BC Emissions Inventory (CARB-EI), BAAQMD's $PM_{2.5}$ Emissions Inventory (BAAQMD-EI), and CMB-EC and $^{14}C$-EC analysis for (A) winter and (B) non-winter samples.

rural site Aspvreten, Sweden). The Asian studies do not have a consistent pattern for winter versus non-winter measurements.

There are only two reported studies to compare for the contiguous U.S., which reflect very different emission scenarios. Although both studies represent urban metropolitan areas, the Bay Area results reported here have a much higher contribution from biomass burning than Salt Lake City, Utah (Mouteva et al., 2017). This may partially reflect differences in urban air quality strategies for the two regions. The Bay Area has been reducing fossil sources, including diesel exhaust, through environmental policy while Salt Lake City is currently working on effective strategies to reduce the recent increases in wintertime $PM_{2.5}$.

## 4. Conclusion

This study provides a detailed description of the sources and seasonal trends for carbonaceous aerosols in the San Francisco Bay Area, including inter-comparison across two receptor-based EC apportionments techniques, two emissions inventories, and a comparison to global studies of $^{14}C$ -based EC apportionment. The two receptor-based techniques ($^{14}C$ and CMB) were very similar on average, although individual sites had larger differences. Of the seven cities included in this study, San Francisco and Napa were the most different in terms of source contributions. Napa had the highest EC mass concentration (winter and non-winter: 1.34 and 0.40 $\mu g\, m^{-3}$, respectively) for both seasons, and a significantly higher contribution from biomass burning than the other sites in winter ($^{14}C$ and CMB: 63 and 75%, respectively). In Napa, enhancement of aerosols in the winter is influenced by both meteorology and change of emission sources (i.e. increased residential wood burning). EC in San Francisco is mainly from fossil fuel combustion for both seasons, ($^{14}C$ and CMB: both 65%). For the remaining four sites (Concord, San Pablo, San Rafael, and Cupertino) EC concentrations and source contributions are similar for the non-winter, but Cupertino has a much lower EC concentration in the winter. For San Francisco and these four sites, unlike Napa, the similar fractions of contemporary and biomass burning contributions during the two seasons suggest that seasonal variation in concentrations is largely driven by meteorology.

Although the receptor-based EC source apportionment techniques had similar results for the split between biomass burning and fossil fuel combustion, there was a larger difference between the receptor-based versus the emissions inventories. Average biomass burning contribution from both emissions inventories is 19% which under predicts receptor-based results by 27% and 35% for $^{14}C$ and CMB, respectively. Contribution of diesel sources in both emissions inventories (including off-road mobile from CARB-EI) has an estimated average contribution of 49% which over predicts receptor-based CMB results by 27%. These results suggest that current EIs have not yet sufficiently accounted for the reductions in EC from diesel emissions that have resulted from improvements in diesel engines and cleaner fuels. Another potential reason may be inherent differences in bottom-up and top-down approaches: EIs account for a comprehensive set of emissions in a

**Table 2**
Compilation of literature values of contribution of biomass burning (%BB) of EC or BC carbonaceous fraction. Sampling location, sampling period and method of EC or BC isolation also included. Arctic and near-Artic studies are listed in a separate section at the end of the table.

| Location | City | Manuscript | %BB - W | %BB - NW | %BB - annual | Sampling Period | EC/BC Isolation |
|---|---|---|---|---|---|---|---|
| ***Asia*** | | | | | | | |
| China | Beijing [a] | Andersson et al., 2015 | 26 [j] | | | Winter 2013 | NIOSH [o] |
| | | Zhang et al., 2015a | 18–28 [j] | | | Winter 2013 | Swiss_4S |
| | | Zhang et al., 2015b * | 24 | 19 | 21 ± 6 | 2010 to 2011 | Swiss_4S |
| | | Chen et al., 2013 | 17 ± 4 | | | Winter 2009–2010 | NIOSH [o] |
| | Shanghai [a] | Andersson et al., 2015 | 32 [j] | | | Winter 2013 | NIOSH [o] |
| | | Zhang et al., 2015a | 21–23 [j] | | | Winter 2013 | Swiss_4S |
| | | Chen et al., 2013 * | 17 ± 4 | | | Winter 2009–2010 | NIOSH [o] |
| | Guangzhou [a] | Andersson et al., 2015 | 32 [j] | | | Winter 2013 | NIOSH [o] |
| | | Zhang et al., 2015a | 19–43 [j] | | | Winter 2013 | Swiss_4S |
| | | Liu et al., 2014 * | 29 ± 10 [j] | | | Winter 2012–2013 | Theodore [p] |
| | Xiamen [a] | Chen et al., 2013 * | 13 ± 3 | | | Winter 2009–2010 | NIOSH [o] |
| | Xi'an [a] | Zhang et al., 2015a * | 22 [j] | | | Winter 2013 | Swiss_4S |
| | Xinxiang [a] | Liu et al., 2017 * | 20 ± 1 | 14 ± 1 [k] | 19 ± 3 | 2013–2014 | multi-methods [p] |
| | Ningbo [b] | Liu et al., 2013 * | 12 | 40 [k] | 22 | 2009–2010 | Theodore [p] |
| | Hainan Island [b] | Zhang et al., 2014 * | | | 62 ± 11 | 2005–2006 | Swiss_4S |
| | Shinglin Bay [b] | Chen et al., 2013 * | 22 ± 3 | | | Winter 2009–2010 | NIOSH [o] |
| South Korea | Jeju Island [b] | Zhang et al., 2016 * | 31 ± 12 | 21 ± 10 | 24 ± 11 | 2013–2014 | Swiss_4S |
| | | Chen et al., 2013 | | 25 ± 6 [l] | | Spring 2011 | NIOSH [o] |
| Japan | Tokyo [a] | Uchida et al., 2010 | 24–28 | 39–42 [k] | | 2002–2004 | CTO-375 |
| | Okinawa [b] | Handa et al., 2010 | | 69 [l, r] | | Spring 2008 | CTO-375 |
| India | Sinhagad [b] | Budhavant et al., 2015 * | 56 ± 3 | 48 ± 8 | | 2008–2009 | NIOSH [o] |
| | | Sheesley et al., 2012 | | | 59 ± 5 | 2008–2009 | CTO-375 |
| | | Gustafsson et al., 2009 | 54 | | | Winter 2006 | NIOSH [o] |
| Maldives | Hanimaadhoo b | Bosch et al., 2014 | 59 ± 4 | | | Winter 2012 | NIOSH [o] |
| | | Budhavant et al., 2015 * | 53 ± 5 | 53 ± 11 | | 2008–2009 | NIOSH [o] |
| | | Sheesley et al., 2012 | | | 73 ± 6 | 2008–2009 | CTO-375 |
| | | Gustafsson et al., 2009 | 41 | | | Winter 2006 | NIOSH [o] |
| Himalaya- | Mustang Valley [d] | Li et al., 2016 * | | | 51–77 | 2013–2014 | NIOSH [o] |
| Tibet | Langtang Valley [e] | Li et al., 2016 * | | | 30–42 | 2013–2014 | NIOSH [o] |
| ***Europe*** | | | | | | | |
| Spain | Barcelona [a] | Minguillón et al., 2011 | 13 ± 1 | 9 ± 1 [k] | | 2009 | Theodore [p] |
| | Montseny [b] | Minguillón et al., 2011 | 34 ± 3 | 21 ± 4 [k] | | 2009 | Theodore [p] |
| United Kingdom | Birmingham [a] | Heal et al., 2011 | | | 7 | 2007–2008 | Theodore [p] |
| Netherlands | Rotterdam [a, f] | Keuken et al., 2013 | | 17 [k] | | Summer 2011 | Theodore [p] |
| Switzerland | Zurich [a] | Zhang et al., 2013 | 36 | | | Winter 2008 | Swiss_4S |
| | | Szidat et al., 2006 * | 25 ± 5 | 6 ± 2 [k] | | 2002–2003 | Theodore [p] |
| | Bern [a] | Zhang et al., 2013 * | | 9 [k] | | Summer 2009 | Swiss_4S |
| | North of Alps [g] | Zotter et al. 2014a* | 42 ± 13 [j] | | | Winter 2008–2012 | Swiss_4S |
| | Roveredo [a] | Sandradewi et al., 2008 | 51 | | | Winter 2005 | Theodore |
| | | Szidat et al., 2007 | 38–71 | 27–73 [l] | | 2005 | Theodore [p] |
| | | Zhang et al., 2013 * | 63 | | | Winter 2005 | Theodore [p] |
| | Moleno [a] | Szidat et al., 2007 | 4–18 | | | Winter 2005 | Theodore [p] |
| | | Zhang et al., 2013 * | | 8 [k] | | Summer 2005 | Theodore [p] |
| | South of Alps [h] | Zotter et al. 2014a * | 49 ± 15 [j] | | | Winter 2008–2012 | Swiss_4S |
| Italy | Milan [a] | Bernardoni et al., 2013 * | 16 | | | Winters 2009–2011 | Theodore [p] |
| Sweden | Stockholm [a] | Andersson et al., 2011 * | 43 ± 23 | 35 ± 18 [m] | | 2006–2007 | CTO-375 |
| | | Zencak et al., 2007 | 70–79 | | | Winter 2005 | CTO-375 |
| | Råö [b] | Szidat et al., 2009 | 30–36 | | | Winter 2005 | Theodore [p] |
| | Aspvreten [b] | Andersson et al., 2011 * | 38 ± 20 | 45 ± 10 [m] | | 2006–2007 | CTO-375 |
| | | Zencak et al., 2007 | 88–99 | | | Winter 2005 | CTO-375 |
| | Göteborg [a] | Szidat et al., 2009 | 7–13 | 3–16 [k] | | 2005–2006 | Theodore [p] |
| Lithuania | Preila [c] | Ulevicius et al., 2016 * | | 67 ± 3 [l, n] | | Spring 2014 | Swiss_4S |
| ***United States*** | | | | | | | |
| California | Bethel Island [b] | This study | 53 ± 6 | 45 ± 10 | 49 ± 6 | 2011–2012 | IMPROVE [o] |
| | Concord [a] | This study | 53 ± 7 | 38 ± 11 | 46 ± 11 | 2011–2012 | IMPROVE [o] |
| | San Pablo [a] | This study | 42 ± 7 | 45 ± 14 | 44 ± 2 | 2011–2012 | IMPROVE [o] |
| | San Rafael [a] | This study | 44 ± 8 | 44 ± 8 | 44 ± 1 | 2011–2012 | IMPROVE [o] |
| | San Francisco [a] | This study | 39 ± 7 | 32 ± 13 | 36 ± 5 | 2011–2012 | IMPROVE [o] |
| | Napa [a] | This study | 63 ± 9 | 43 ± 8 | 53 ± 14 | 2011–2012 | IMPROVE [o] |
| | Cupertino [a] | This study | 44 ± 5 | 38 ± 10 | 41 ± 4 | 2011–2012 | IMPROVE [o] |
| | avg of Bay Area, CA | This study * | 48 ± 8 | 41 ± 5 | 45 ± 6 | 2011–2012 | IMPROVE [o] |
| Utah | Salt Lake City [a, i] | Mouteva et al., 2017 * | 12 | 8 [k] | 11 | 2012–2013 | Swiss_4S |
| ***Artic/sub-Artic*** | | | | | | | |
| Alaska, US | Barrow [c] | Barrett et al., 2015 * | 32 ± 9 | 51 ± 6 [l] | | Winter 2012–2013 | NIOSH [o] |
| | Interior Alaska [s] | Mouteva et al., 2015 | | −10 – +106 ‰ [s, n] | | Summer 2013 | Swiss_4S |
| | Interior Alaska [s] | Mouteva et al., 2015 | | −354 – -57 ‰ [s] | | Summer 2013 | Swiss_4S |

(*continued on next page*)

**Table 2** (*continued*)

| Location | City | Manuscript | %BB - W | %BB - NW | %BB - annual | Sampling Period | EC/BC Isolation |
|---|---|---|---|---|---|---|---|
| Norway | Svalbard [c] | Winiger et al., 2015 * | 52 ± 15 [j] | | | Winter 2009 | NIOSH [o] |
| Russia | Tiksi [c] | Winiger et al., 2017 * | 19 ± 3 | 73 ± 5 [k] | 31 ± 19 | 2012–2014 | NIOSH [o] |
| Sweden | Abisko [c] | Winiger et al., 2016 * | 17–47 | 58 ± 22 [l, k] | 42 ± 15 | 2011–2013 | NIOSH [o] |

[a] urban site. [b] rural site. [c] remote site. [d] average of four sampling sites: Zhongba, Jomsom, Pokhara, and Lumbini. [e] average of five sampling sites: Kathmandu, Dhunche, Nyalam, Lhasa, and Namco. [f] average of three sites in Rotterdam: edge of residential area north, south of city, and on a center city street. [g] average of eleven sites north of the Alps. [h] average of five sites south of the Alps. [i] average of three sites in Salt Lake City: urban site, industrial site, suburban site. [j] high pollution event/smog event. [k] summer season. [l] spring season or late winter. [m] autumn season. [n] biomass burning event. [o] using the split-time from this run method to volatilize the OC and isolate EC. [p] modified Theodore method which can include a water extraction and varying modifications to the temperature and run time. (Szidat et al., 2004a,b) [q] He-200, He-EUSSAR_2, and He/O2-300. [r] average reported as percent modern carbon study [s] includes measurements from two sampling sites (Fairbanks and Delta Junction) and reports findings as **Δ** $^{14}$C value (per mil). *measurement from study included in Fig. 8 and Figure S1.

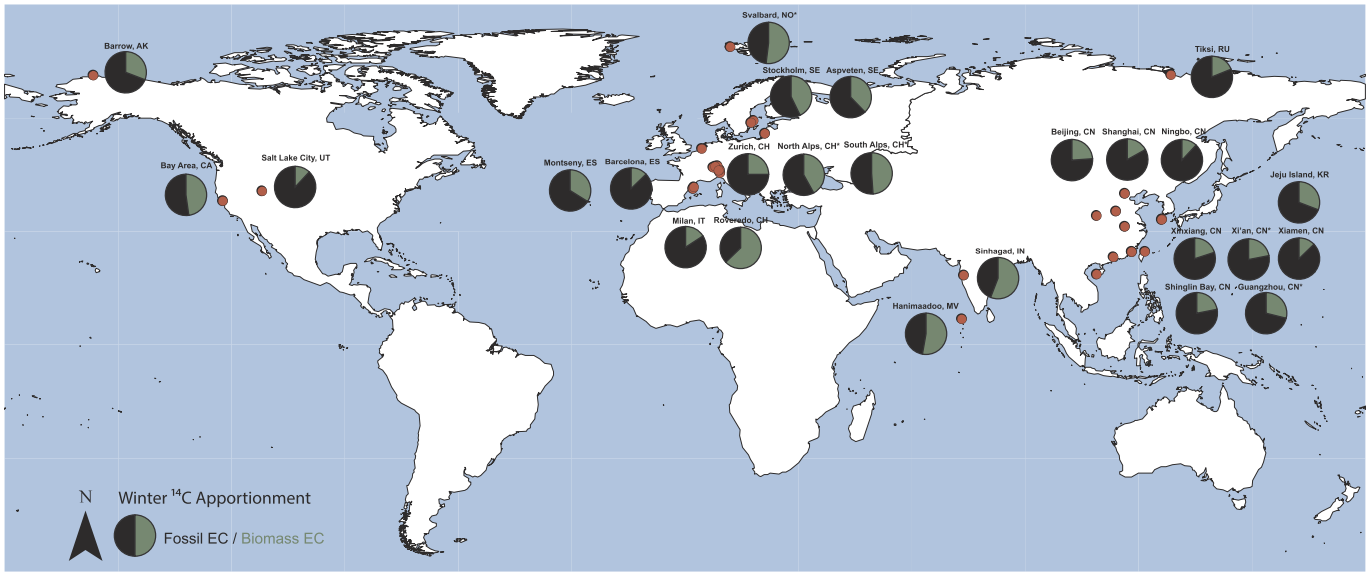


**Fig. 8.** Global map of biomass burning and fossil fuel contribution of winter EC or BC values from radiocarbon-based source apportionment studies. The studies included in the figure have reported average winter values. *samples collected during high pollution/haze or biomass burning events. Table 2 includes all references.

specified area and time while receptor-based ambient aerosol measurements will represent all aerosol, whether emitted within the EI region or transported from another region. However, transport of biomass burning EC into the Bay Area from outside of California (therefore outside of the EIs), maybe partially responsible for the observed higher biomass burning contribution to EC. Even so, based on this study the Bay Area will require emission reductions specific to the samples. Additional biomass burning regulations would most improve air quality in Napa, while more stringent motor vehicle regulations would have the largest impact in San Francisco.

Though it has been established that EC (or BC) concentrations have been decreasing across the US in the last several decades (Kirchstetter et al., 2017), results of the current study and the accumulated global studies indicate that in developed countries with intense air pollution regulations, biomass burning may be increasingly important for ambient EC concentrations. With the variation reported for the U.S. and Europe, continued characterization of EC, including source apportionment by $^{14}$C, is needed in the U.S. to evaluate the efficacy of pollution control strategies and to continue to reduce PM pollution in urban, rural and remote regions.

## Funding

This work was supported by the Bay Area Air Quality Management District [contract numbers 2013.075 and 2015.160]. Publication was made possible, in part, by support from the Open Access Fund sponsored by the Baylor University Libraries. We also thank Thomas W. Kirchstetter and Xiaochen Tang at Lawrence Berkeley National Laboratory for providing pinewood source samples used in this study.

## Declaration of interest

None.

## Appendix A. Supplementary data

Supplementary data to this article can be found online at https://doi.org/10.1016/j.atmosenv.2018.09.050.

## References

Andersson, A., Sheesley, R.J., Kruså, M., Johansson, C., Gustafsson, Ö., 2011. 14C-Based source assessment of soot aerosols in Stockholm and the Swedish EMEP-Aspvreten regional background site. Atmos. Environ. 45, 215–222.
Andersson, A., Deng, J., Du, K., Zheng, M., Yan, C., Sköld, M., Gustafsson, O. r., 2015. Regionally-varying combustion sources of the January 2013 severe haze events over eastern China. Environ. Sci. Technol. 49, 2038–2043.
Bahadur, R., Feng, Y., Russell, L.M., Ramanathan, V., 2011. Impact of California's air pollution laws on black carbon and their implications for direct radiative forcing. Atmos. Environ. 45, 1162–1167.
Barbero, R., Abatzoglou, J., Larkin, N., Kolden, C., Stocks, B., 2015. Climate change presents increased potential for very large fires in the contiguous United States. Int. J. Wildland Fire 24, 892–899.
Barrett, T., Robinson, E., Usenko, S., Sheesley, R., 2015. Source contributions to wintertime elemental and organic carbon in the western arctic based on radiocarbon and

tracer apportionment. Environ. Sci. Technol. 49, 11631–11639.
Bernardoni, V., Calzolai, G., Chiari, M., Fedi, M., Lucarelli, F., Nava, S., Piazzalunga, A., Riccobono, F., Taccetti, F., Valli, G., 2013. Radiocarbon analysis on organic and elemental carbon in aerosol samples and source apportionment at an urban site in Northern Italy. J. Aerosol Sci. 56, 88–99.
Bond, T.C., Streets, D.G., Yarber, K.F., Nelson, S.M., Woo, J.H., Klimont, Z., 2004. A technology-based global inventory of black and organic carbon emissions from combustion. J. Geophys. Res. 109. https://doi.org/10.1029/2003JD003697.
Bosch, C., Andersson, A., Kirillova, E.N., Budhavant, K., Tiwari, S., Praveen, P., Russell, L.M., Beres, N.D., Ramanathan, V., Gustafsson, Ö., 2014. Source-diagnostic dual-isotope composition and optical properties of water-soluble organic carbon and elemental carbon in the South Asian outflow intercepted over the Indian Ocean. J. Geophys. Res. 119 (11) 743-711,759.
Briggs, N.L., Long, C.M., 2016. Critical review of black carbon and elemental carbon source apportionment in Europe and the United States. Atmos. Environ. 144, 409–427.
Budhavant, K., Andersson, A., Bosch, C., Kruså, M., Kirillova, E., Sheesley, R., Safai, P., Rao, P., Gustafsson, Ö., 2015. Radiocarbon-based source apportionment of elemental carbon aerosols at two South Asian receptor observatories over a full annual cycle. Environ. Res. Lett. 10, 064004.
California Air Resources Board (CARB), 2016. CARB Black Carbon Emission Inventory Technical Support Document.
California Department of Forestry and Fire Protection (CAL FIRE), 2012. 2012 Wildfire Activity Statistics. http://www.fire.ca.gov/downloads/redbooks/2012Redbook/2012_Redbook_Complete.pdf.
Cao, G., Zhang, X., Gong, S., An, X., Wang, Y., 2011a. Emission inventories of primary particles and pollutant gases for China. Chin. Sci. Bull. 56, 781.
Cao, J.-j., Chow, J.C., Tao, J., Lee, S.-c., Watson, J.G., Ho, K.-f., Wang, G.-h., Zhu, C.-s., Han, Y.-m., 2011b. Stable carbon isotopes in aerosols from Chinese cities: influence of fossil fuels. Atmos. Environ. 45, 1359–1363.
Chen, B., Andersson, A., Lee, M., Kirillova, E.N., Xiao, Q., Kruså, M., Shi, M., Hu, K., Lu, Z., Streets, D.G., 2013. Source forensics of black carbon aerosols from China. Environ. Sci. Technol. 47, 9102–9108.
Chow, J.C., Watson, J.G., Pritchett, L.C., Pierson, W.R., Frazier, C.A., Purcell, R.G., 1993. The DRI thermal/optical reflectance carbon analysis system: description, evaluation and applications in US air quality studies. Atmos. Environ. 27, 1185–1201.
Chow, J.C., Watson, J.G., Crow, D., Lowenthal, D.H., Merrifield, T., 2001. Comparison of IMPROVE and NIOSH carbon measurements. Aerosol Sci. Technol. 34, 23–34.
Chow, J.C., Watson, J.G., Lowenthal, D.H., Chen, L.-W.A., Motallebi, N., 2010. Black and organic carbon emission inventories: review and application to California. J. Air Waste Manag. Assoc. 60, 497–507.
Claire, S.J., Dinh, T.M., Fanai, A.K., Nguyen, M.H., Schultz, S.A., 2015. Bay Area Emissions Inventory Summary Report: Greenhouse Gases. Base Year 2011. Bay Area Air Quality Management District.
Dallmann, T.R., Harley, R.A., Kirchstetter, T.W., 2011. Effects of diesel particle filter retrofits and accelerated fleet turnover on drayage truck emissions at the Port of Oakland. Environ. Sci. Technol. 45, 10773–10779. https://doi.org/10.1021/es202609q.
Dallmann, T.R., Kirchstetter, T.W., DeMartini, S.J., Harley, R.A., 2013. Quantifying on-road emissions from gasoline-powered motor vehicles: accounting for the presence of medium- and heavy-duty diesel trucks. Environ. Sci. Technol. 47, 13873–13881. https://doi.org/10.1021/es402875u.
Dusek, U., Monaco, M., Prokopiou, M., Gongriep, F., Hitzenberger, R., Meijer, H., Röckmann, T., 2014. Evaluation of a 2-step thermal method for separating organic and elemental carbon for radiocarbon analysis. Atmos. Meas. Tech. 7, 131–169.
Fairley, D., 2012. Sources of Bay Area Fine Particles: 2010 Update and Trends.
Fairley, D., 2014. Wood-burning Devices in the San Francisco Bay Area-update. Bay Area Air Qualtiy Management Office Memorandum.
Fanai, A.K., Claire, S.J., Dinh, T.M., Nguyen, T.H., Schultz, S.A., 2014. Bay Area Emissions Inventory Summary Report: Criteria Air Pollutants. Base Year 2011. Bay Area Air Quality Management District.
Fraser, M., Yue, Z., Buzcu, B., 2003. Source apportionment of fine particulate matter in Houston, TX, using organic molecular markers. Atmos. Environ. 37, 2117–2123.
Glen, W.G., Zelenka, M.P., Graham, R.C., 1996. Relating meteorological variables and trends in motor vehicle emissions to monthly urban carbon monoxide concentrations. Atmos. Environ. 30, 4225–4232.
Gustafsson, Ö., Kruså, M., Zencak, Z., Sheesley, R.J., Granat, L., Engström, E., Praveen, P., Rao, P., Leck, C., Rodhe, H., 2009. Brown clouds over South Asia: biomass or fossil fuel combustion? Science 323, 495–498.
Handa, D., Nakajima, H., Arakaki, T., Kumata, H., Shibata, Y., Uchida, M., 2010. Radiocarbon analysis of BC and OC in PM10 aerosols at Cape Hedo, Okinawa, Japan, during long-range transport events from East Asian countries. Nucl. Instrum. Methods Phys. Res. Sect. B Beam Interact. Mater. Atoms 268, 1125–1128.
Heal, M.R., Naysmith, P., Cook, G.T., Xu, S., Duran, T.R., Harrison, R.M., 2011. Application of 14C analyses to source apportionment of carbonaceous PM2. 5 in the UK. Atmos. Environ. 45, 2341–2348.
Huang, R.-J., Zhang, Y., Bozzetti, C., Ho, K.-F., Cao, J.-J., Han, Y., Daellenbach, K.R., Slowik, J.G., Platt, S.M., Canonaco, F., 2014. High secondary aerosol contribution to particulate pollution during haze events in China. Nature 514, 218.
Keuken, M., Moerman, M., Voogt, M., Blom, M., Weijers, E., Röckmann, T., Dusek, U., 2013. Source contributions to PM2. 5 and PM10 at an urban background and a street location. Atmos. Environ. 71, 26–35.
Kirchstetter, T.W., Harley, R.A., Kreisberg, N.M., Stolzenburg, M.R., Hering, S.V., 1999. On-road measurement of fine particle and nitrogen oxide emissions from light-and heavy-duty motor vehicles. Atmos. Environ. 33, 2955–2968.
Kirchstetter, T.W., Aguiar, J., Tonse, S., Fairley, D., Novakov, T., 2008a. Black carbon concentrations and diesel vehicle emission factors derived from coefficient of haze measurements in California: 1967–2003. Atmos. Environ. 42, 480–491.
Kirchstetter, T.W., Agular, J., Tonse, S., Fairley, D., Novakov, T., 2008b. Black carbon concentrations and diesel vehicle emission factors derived from coefficient of haze measurements in California: 1967-2003. Atmos. Environ. 42, 480–491. https://doi.org/10.1016/j.atmosenv.2007.09.063.
Kirchstetter, T.W., Preble, C.V., Hadley, O.L., Bond, T.C., Apte, J.S., 2017. Large reductions in urban black carbon concentrations in the United States between 1965 and 2000. Atmos. Environ. 151, 17–23.
Kleindienst, T.E., Jaoui, M., Lewandowski, M., Offenberg, J.H., Lewis, C.W., Bhave, P.V., Edney, E.O., 2007. Estimates of the contributions of biogenic and anthropogenic hydrocarbons to secondary organic aerosol at a southeastern US location. Atmos. Environ. 41, 8288–8300. https://doi.org/10.1016/j.atmosenv.2007.06.045.
Lewis, C.W., Klouda, G.A., Ellenson, W.D., 2004. Radiocarbon measurement of the biogenic contribution to summertime PM-2.5 ambient aerosol in Nashville. TN. Atmos. Environ. 38, 6053–6061.
Li, C., Bosch, C., Kang, S., Andersson, A., Chen, P., Zhang, Q., Cong, Z., Chen, B., Qin, D., Gustafsson, Ö., 2016. Sources of black carbon to the Himalayan–Tibetan Plateau glaciers. Nat. Commun. 7, 12574.
Liu, D., Li, J., Zhang, Y., Xu, Y., Liu, X., Ding, P., Shen, C., Chen, Y., Tian, C., Zhang, G., 2013. The use of levoglucosan and radiocarbon for source apportionment of PM2. 5 carbonaceous aerosols at a background site in East China. Environ. Sci. Technol. 47, 10454–10461.
Liu, J., Li, J., Zhang, Y., Liu, D., Ding, P., Shen, C., Shen, K., He, Q., Ding, X., Wang, X., 2014. Source apportionment using radiocarbon and organic tracers for PM2. 5 carbonaceous aerosols in Guangzhou, South China: contrasting local-and regional-scale haze events. Environ. Sci. Technol. 48, 12002–12011.
Liu, J., Li, J., Ding, P., Zhang, Y., Liu, D., Shen, C., Zhang, G., 2017. Optimizing isolation protocol of organic carbon and elemental carbon for 14C analysis using fine particulate samples. Atmos. Environ. 154, 9–19.
Lough, G.C., Christensen, C.G., Schauer, J.J., Tortorelli, J., Mani, E., Lawson, D.R., Clark, N.N., Gabele, P.A., 2007. Development of molecular marker source profiles for emissions from on-road gasoline and diesel vehicle fleets. J. Air Waste Manag. Assoc. 57, 1190–1199.
Mclarney, T., Sarles, R., 2005. Spare the Air Tonight Study: 2005-2006 Winter Wood Smoke Season. True North Research, Inc Published by the Bay Area Air Quality Management District.
Malone, D., Basso, M., Nguyen, D., 2013. 2012 Air Monitoring Network Plan. Bay Area Air Quality Management District.
Minguillón, M., Perron, N., Querol, X., Szidat, S., Fahrni, S., Alastuey, A., Jimenez, J., Mohr, C., Ortega, A., Day, D., 2011. Fossil versus contemporary sources of fine elemental and organic carbonaceous particulate matter during the DAURE campaign in Northeast Spain. Atmos. Chem. Phys. 11, 12067–12084.
Mohn, J., Szidat, S. n., Fellner, J., Rechberger, H., Quartier, R., Buchmann, B., Emmenegger, L., 2008. Determination of biogenic and fossil CO 2 emitted by waste incineration based on 14 CO 2 and mass balances. Bioresour. Technol. 99, 6471–6479.
Mohr, C., Huffman, J.A., Cubison, M.J., Aiken, A.C., Docherty, K.S., Kimmel, J.R., Ulbrich, I.M., Hannigan, M., Jimenez, J.L., 2009. Characterization of primary organic aerosol emissions from meat cooking, trash burning, and motor vehicles with high-resolution aerosol mass spectrometry and comparison with ambient and chamber observations. Environ. Sci. Technol. 43, 2443–2449.
Mouteva, G., Czimczik, C.I., Fahrni, S.M., Wiggins, E., Rogers, B.M., Veraverbeke, S., Xu, X., Santos, G., Henderson, J., Miller, C., 2015. Black carbon aerosol dynamics and isotopic composition in Alaska linked with boreal fire emissions and depth of burn in organic soils. Global Biogeochem. Cycles 29, 1977–2000.
Mouteva, G.O., Randerson, J.T., Fahrni, S.M., Bush, S.E., Ehleringer, J.R., Xu, X., Santos, G.M., Kuprov, R., Schichtel, B.A., Czimczik, C.I., 2017. Using radiocarbon to constrain black and organic carbon aerosol sources in Salt Lake City. J. Geophys. Res. 122, 9843–9857. https://doi.org/10.1002/2017JD026519.
Riley, K.L., Abatzoglou, J.T., Grenfell, I.C., Klene, A.E., Heinsch, F.A., 2013. The relationship of large fire occurrence with drought and fire danger indices in the western USA, 1984–2008: the role of temporal scale. Int. J. Wildland Fire 22, 894–909.
Rinehart, L.R., Fujita, E.M., Chow, J.C., Magliano, K., Zielinska, B., 2006. Spatial distribution of PM2. 5 associated organic compounds in central California. Atmos. Environ. 40, 290–303.
Rogge, W.F., Hildemann, L.M., Mazurek, M.A., Cass, G.R., Simoneit, B.R., 1991. Sources of fine organic aerosol. 1. Charbroilers and meat cooking operations. Environ. Sci. Technol. 25, 1112–1125.
Sandradewi, J., Prévôt, A.S., Szidat, S., Perron, N., Alfarra, M.R., Lanz, V.A., Weingartner, E., Baltensperger, U., 2008. Using aerosol light absorption measurements for the quantitative determination of wood burning and traffic emission contributions to particulate matter. Environ. Sci. Technol. 42, 3316–3323.
Schauer, J.J., Cass, G.R., 2000. Source apportionment of wintertime gas-phase and particle-phase air pollutants using organic compounds as tracers. Environ. Sci. Technol. 34, 1821–1832.
Schauer, J.J., Rogge, W.F., Hildemann, L.M., Mazurek, M.A., Cass, G.R., Simoneit, B.R., 1996. Source apportionment of airborne particulate matter using organic compounds as tracers. Atmos. Environ. 30, 3837–3855.
Sheesley, R.J., Kirillova, E., Andersson, A., Krusa, M., Praveen, P.S., Budhavant, K., Safai, P.D., Rao, P.S.P., Gustafsson, O., 2012. Year-round radiocarbon-based source apportionment of carbonaceous aerosols at two background sites in South Asia. J. Geophys. Res. 117. https://doi.org/10.1029/2011JD017161.
Slater, J., Currie, L.A., Dibb, J.E., Benner, B., 2002. Distinguishing the relative contribution of fossil fuel and biomass combustion aerosols deposited at Summit, Greenland through isotopic and molecular characterization of insoluble carbon.

Atmos. Environ. 36, 4463–4477.
Stone, E.A., Schauer, J.J., Pradhan, B.B., Dangol, P.M., Habib, G., Venkataraman, C., Ramanathan, V., 2010. Characterization of emissions from South Asian biofuels and application to source apportionment of carbonaceous aerosol in the Himalayas. J. Geophys. Res. 115.
Strader, R., Lurmann, F., Pandis, S.N., 1999. Evaluation of secondary organic aerosol formation in winter. Atmos. Environ. 33, 4849–4863.
Stuiver, M., Polach, H.A., 1977. Discussion; reporting of C-14 data. Radiocarbon 19, 355–363.
Szidat, S., Jenk, T., Gäggeler, H., Synal, H.-A., Fisseha, R., Baltensperger, U., Kalberer, M., Samburova, V., Wacker, L., Saurer, M., 2004a. Source apportionment of aerosols by 14 C measurements in different carbonaceous particle fractions. Radiocarbon 46, 475–484.
Szidat, S., Jenk, T., Gäggeler, H., Synal, H.-A., Hajdas, I., Bonani, G., Saurer, M., 2004b. THEODORE, a two-step heating system for the EC/OC determination of radiocarbon (14C) in the environment. Nucl. Instrum. Methods Phys. Res. Sect. B Beam Interact. Mater. Atoms 223, 829–836.
Szidat, S., Jenk, T.M., Synal, H.A., Kalberer, M., Wacker, L., Hajdas, I., Kasper-Giebl, A., Baltensperger, U., 2006. Contributions of fossil fuel, biomass-burning, and biogenic emissions to carbonaceous aerosols in Zurich as traced by 14C. J. Geophys. Res. 111.
Szidat, S., Prévôt, A.S., Sandradewi, J., Alfarra, M.R., Synal, H.A., Wacker, L., Baltensperger, U., 2007. Dominant impact of residential wood burning on particulate matter in Alpine valleys during winter. Geophys. Res. Lett. 34.
Szidat, S., Ruff, M., Perron, N., Wacker, L., Synal, H.-A., Hallquist, M., Shannigrahi, A.S., Yttri, K.E., Dye, C., Simpson, D., 2009. Fossil and non-fossil sources of organic carbon (OC) and elemental carbon (EC) in Göteborg, Sweden. Atmos. Chem. Phys. 9, 1521–1535.
Turpin, B.J., Huntzicker, J.J., 1995. Identification of secondary organic aerosol episodes and quantitation of primary and secondary organic aerosol concentrations during SCAQS. Atmos. Environ. 29, 3527–3544.
Turpin, B.J., Huntzicker, J.J., Larson, S.M., Cass, G.R., 1991. Los Angeles summer midday particulate carbon: primary and secondary aerosol. Environ. Sci. Technol. 25, 1788–1793.
Uchida, M., Kumata, H., Koike, Y., Tsuzuki, M., Uchida, T., Fujiwara, K., Shibata, Y., 2010. Radiocarbon-based source apportionment of black carbon (BC) in PM10 aerosols from residential area of suburban Tokyo. Nucl. Instrum. Methods Phys. Res. Sect. B Beam Interact. Mater. Atoms 268, 1120–1124.
Ulevicius, V., Byčenkienė, S., Bozzetti, C., Vlachou, A., Plauškaitė, K., Mordas, G., Dudoitis, V., Abbaszade, G., Remeikis, V., Garbaras, A., 2016. Fossil and non-fossil source contributions to atmospheric carbonaceous aerosols during extreme spring grassland fires in Eastern Europe. Atmos. Chem. Phys. 16, 5513–5529.
U.S. Census Bureau, 2012a. California: 2010 Population and Housing Unit Counts. https://www.census.gov/prod/cen2010/cph-2-6.pdf.
U.S. Census Bureau, 2012b. Geographic Terms and Concepts- Core Based Statistical Areas and Related Statistical Areas. https://www.census.gov/geo/reference/gtc/gtc_cbsa.html.
Westerling, A.L., Hidalgo, H.G., Cayan, D.R., Swetnam, T.W., 2006. Warming and earlier spring increase western US forest wildfire activity. Science 313, 940–943.
Winiger, P., Andersson, A., Yttri, K.E., Tunved, P., Gustafsson, O. r., 2015. Isotope-based source apportionment of EC aerosol particles during winter high-pollution events at the Zeppelin Observatory, Svalbard. Environ. Sci. Technol. 49, 11959–11966.
Winiger, P., Andersson, A., Eckhardt, S., Stohl, A., Gustafsson, Ö., 2016. The sources of atmospheric black carbon at a European gateway to the Arctic. Nat. Commun. 7, 12776.
Winiger, P., Andersson, A., Eckhardt, S., Stohl, A., Semiletov, I.P., Dudarev, O.V., Charkin, A., Shakhova, N., Klimont, Z., Heyes, C., Gustafsson, Ö., 2017. Siberian Arctic black carbon sources constrained by model and observation. Proc. Natl. Acad. Sci 114, E1054–E1061.
Zencak, Z., Elmquist, M., Gustafsson, Ö., 2007. Quantification and radiocarbon source apportionment of black carbon in atmospheric aerosols using the CTO-375 method. Atmos. Environ. 41, 7895–7906.
Zenker, K., Vonwiller, M., Szidat, S., Calzolai, G., Giannoni, M., Bernardoni, V., Jedynska, A.D., Henzing, B., Meijer, H.A., Dusek, U., 2017. Evaluation and inter-comparison of oxygen-based OC-EC separation methods for radiocarbon analysis of ambient aerosol particle samples. Atmosphere 8, 226.
Zhang, Y., Zotter, P., Perron, N., Prévôt, A., Wacker, L., Szidat, S., 2013. Fossil and non-fossil sources of different carbonaceous fractions in fine and coarse particles by radiocarbon measurement. Radiocarbon 55, 1510–1520.
Zhang, Y.-L., Li, J., Zhang, G., Zotter, P., Huang, R.-J., Tang, J.-H., Wacker, L., Prévôt, A.S., Szidat, S. n., 2014. Radiocarbon-based source apportionment of carbonaceous aerosols at a regional background site on Hainan Island, South China. Environ. Sci. Technol. 48, 2651–2659.
Zhang, Y.-L., Huang, R.-J., El Haddad, I., Ho, K.-F., Cao, J.-J., Han, Y., Zotter, P., Bozzetti, C., Daellenbach, K., Canonaco, F., 2015a. Fossil vs. non-fossil sources of fine carbonaceous aerosols in four Chinese cities during the extreme winter haze episode of 2013. Atmos. Chem. Phys. 15, 1299–1312.
Zhang, Y.-L., Schnelle-Kreis, J. r., Abbaszade, G. l., Zimmermann, R., Zotter, P., Shen, R.-r., Schäfer, K., Shao, L., Prévôt, A.S., Szidat, S. n., 2015b. Source apportionment of elemental carbon in Beijing, China: insights from radiocarbon and organic marker measurements. Environ. Sci. Technol. 49, 8408–8415.
Zhang, Y.-L., Kawamura, K., Agrios, K., Lee, M., Salazar, G., Szidat, S. n., 2016. Fossil and nonfossil sources of organic and elemental carbon aerosols in the outflow from Northeast China. Environ. Sci. Technol. 50, 6284–6292.
Zheng, M., Cass, G.R., Schauer, J.J., Edgerton, E.S., 2002. Source apportionment of PM2.5 in the southeastern United States using solvent-extractable organic compounds as tracers. Environ. Sci. Technol. 36, 2361–2371.
Zotter, P., Ciobanu, V., Zhang, Y., El-Haddad, I., Macchia, M., Daellenbach, K., Salazar, G., Huang, R.-J., Wacker, L., Hueglin, C., 2014a. Radiocarbon analysis of elemental and organic carbon in Switzerland during winter-smog episodes from 2008 to 2012–Part 1: source apportionment and spatial variability. Atmos. Chem. Phys. 14, 13551–13570.
Zotter, P., El-Haddad, I., Zhang, Y., Hayes, P.L., Zhang, X., Lin, Y.H., Wacker, L., Schnelle-Kreis, J., Abbaszade, G., Zimmermann, R., 2014b. Diurnal cycle of fossil and nonfossil carbon using radiocarbon analyses during CalNex. J. Geophys. Res. 119, 6818–6835. https://doi.org/10.1002/2013JD021114.